BENDING FLUTTER AND TORSIONAL FLUTTER OF FLEXIBLE HYDROFOIL STRUTS

Peter K. Besch, et al

Naval Ship Research and Development Center
Bethesda, Maryland

February 1973

NAVAL SHIP RESEARCH AND DEVELOPMENT CENTER

Bethesda, Maryland 20034

BENDING FLUTTER AND TORSIONAL FLUTTER OF FLEXIBLE HYDROFOIL STRUTS

by

Peter K. Besch and Yung-Ming Liu

APPROVED FOR PUBLIC RELEASE; DISTRIBUTION UNLIMITED

SHIP PERFORMANCE DEPARTMENT

RESEARCH AND DEVELOPMENT REPORT

February 1973 Report 4012

BENDING FLUTTER AND TORSIONAL FLUTTER OF FLEXIBLE HYDROFOIL STRUTS

The Naval Ship Research and Development Center is a U. S. Navy center for laboratory effort directed at advancing the state of the art of naval vessels. It was formed in March 1967 by merging the David Taylor Model Basin at Carderock, Maryland with the Marine Engineering Laboratory at Annapolis, Maryland.

Naval Ship Research and Development Center
Bethesda, Md. 20034

MAJOR NSRDC ORGANIZATIONAL COMPONENTS

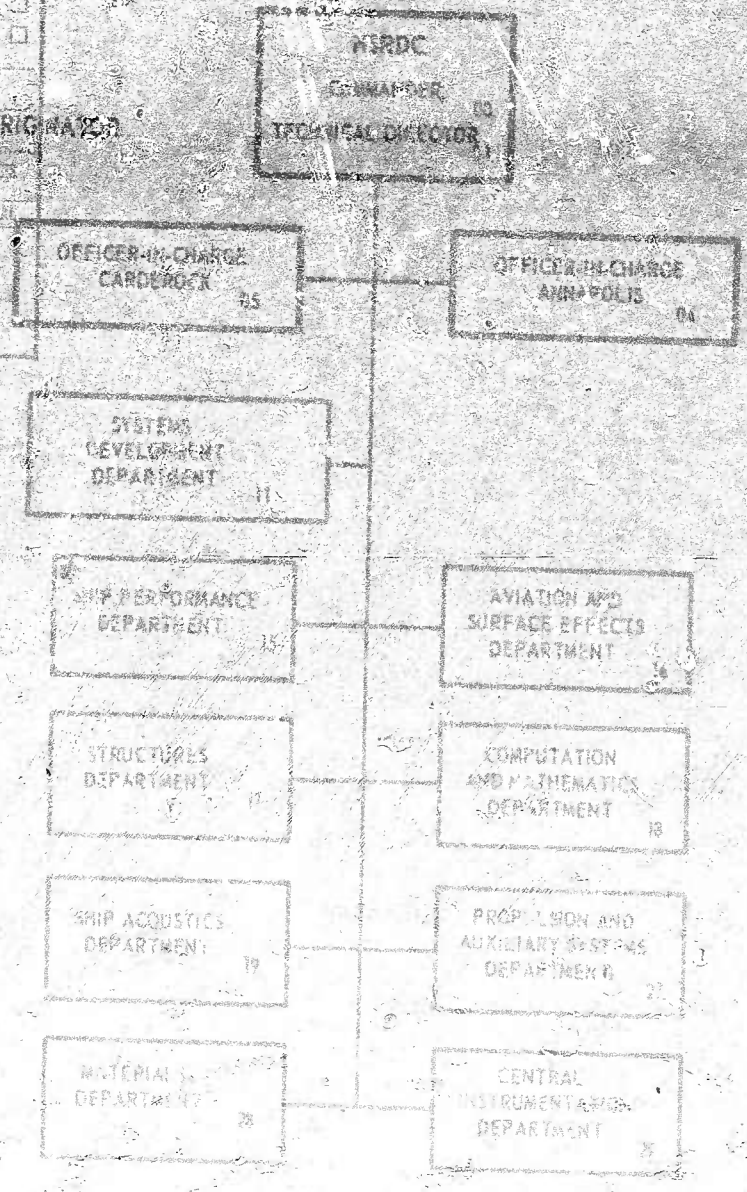

UNCLASSIFIED
Security Classification

DOCUMENT CONTROL DATA - R & D

Security classification of title, body of abstract and indexing annotation must be entered when the overall report is classified)

1. ORIGINATING ACTIVITY (Corporate author)	2a. REPORT SECURITY CLASSIFICATION
Naval Ship Research and Development Center Bethesda, Maryland 20034	UNCLASSIFIED 2b. GROUP

3. REPORT TITLE

BENDING FLUTTER AND TORSIONAL FLUTTER OF FLEXIBLE HYDROFOIL STRUTS

4. DESCRIPTIVE NOTES (Type of report and inclusive dates)

5. AUTHOR(S) (First name, middle initial, last name)

Peter K. Besch and Yuan-Ning Liu

6. REPORT DATE	7a. TOTAL NO. OF PAGES	7b. NO. OF REFS
February 1973	64	22

8a. CONTRACT OR GRANT NO	9a. ORIGINATOR'S REPORT NUMBER(S)
b. PROJECT NO.	4012
c. Subproject S4606 d. Task 1703	9b. OTHER REPORT NO(S) (Any other numbers that may be assigned this report)

10. DISTRIBUTION STATEMENT

APPROVED FOR PUBLIC RELEASE: DISTRIBUTION UNLIMITED

11. SUPPLEMENTARY NOTES	12. SPONSORING MILITARY ACTIVITY
	Naval Ship Systems Command

13. ABSTRACT

A large body of experimental and theoretical flutter results for hydrofoil struts were analyzed to determine significant characteristics. Flutter was found to occur in two different structural mode shapes, corresponding to a predominantly bending mode and a predominantly torsional mode, respectively. The flutter mode shape was related to the vibration mode shapes and the generalized mass ratio of the strut at zero speed. The behavior of the hydroelastic modes of typical struts as a function of speed was investigated by using a strip theory with three-dimensional loading modifications. Flutter predictions for struts which underwent flutter in the torsional mode were usually conservative and predicted the correct mode shape. However, flutter predictions for struts which underwent flutter in the bending mode were unreliable in predicting the mode of flutter because of an extreme sensitivity to the loading modification used. Strut-foil systems of the inverted-T configuration typical of full-scale hydrofoil craft appear to undergo either bending flutter or torsional flutter, depending on pod and foil characteristics.

(Verbatim reproduction of paper presented at Ninth Symposium on Naval Hydrodynamics, 20-25 August 1972, Paris, France)

DD FORM 1 NOV 65 1473 (PAGE 1)

S/N 0101-807-6801

viii

UNCLASSIFIED
Security Classification

14 KEY WORDS	LINK A		LINK B		[illegible]	
	ROLE	WT	ROLE	WT	ROLE	WT
Hydrofoil						
Flutter						
Bending						
Torsional						
Strut						
Vibration						
Flutter						
Bending						
Torsional						
Strut						

DEPARTMENT OF THE NAVY
NAVAL SHIP RESEARCH AND DEVELOPMENT CENTER
BETHESDA, MD. 20034

BENDING FLUTTER AND TORSIONAL FLUTTER OF FLEXIBLE HYDROFOIL STRUTS

by
Peter K. Besch and Yuan-Ning Liu

February 1973 Report 4012

TABLE OF CONTENTS

LIST OF FIGURES

LIST OF TABLES

NOTATION

Symbol	Definition
a	Nondimensional distance from midchord to elastic axis, measured perpendicular to elastic axis, positive aft as fraction of semichord b
a_c	Nondimensional distance from midchord to local aerodynamic center (for steady flow) measured perpendicular to elastic axis, positive aft as a fraction of semichord b
b	Semichord measured perpendicular to elastic axis
$[C]$	Damping matrix of strut
$[C']$	Effective damping matrix of the strut-fluid system
$C(k)$	Complex Theodorsen circulation function
$C_{\ell\alpha}$	Local lift slope for a strip perpendicular to elastic axis in steady flow
EI	Bending stiffness
F	Hydrodynamic force
GJ	Torsional stiffness
g	Structural damping coefficient; also, gravitational acceleration
H	Amplitude of bending displacement h
h	Linear displacement of strut at elastic axis
I_α	Total mass moment of inertia of strut and tip attachments about elastic axis
$I^*_{\alpha,\ pod}$	Added moment of inertia of pod about elastic axis of strut, approximated by the added moment of inertia of a prolate spheroid
j	$\sqrt{-1}$
$[K]$	Stiffness matrix of strut
$[K']$	Effective stiffness matrix of the strut-fluid system
L	Strut length along elastic axis

Symbol	Definition
ℓ	Distance from free surface to tip of strut along elastic axis
M	Oscillatory moment about elastic axis per unit span of strut, positive in direction of positive θ
[M]	Mass matrix of strut
[M*]	Added mass matrix of strut
[M']	Effective mass matrix of the strut-fluid system
m	Mass per unit span along elastic axis
P	Oscillatory lift per unit span of strut along elastic axis, positive in direction of positive h
p	Spanwise modification factor for noncirculatory loading
r_α	Nondimensional radius of gyration
s	Complex eigenvalue
t	Time
V	Flow speed
w	Downwash; vertical component of flow velocity on foil, positive in direction of negative h
x_α	Nondimensional distance from elastic axis to center of gravity, measured perpendicular to elastic axis, positive aft as fraction of semichord b
y	Spanwise coordinate along elastic axis of strut
ζ	Damping ratio, giving damping as a fraction of critical damping
Θ	Amplitude of torsional displacement θ
θ	Torsional displacement of strut about elastic axis, positive when leading edge moves in direction of positive h
κ	Sweep parameter; $(2b \tan \Lambda_{ea})/L$
Λ_{ea}	Elastic-axis sweep angle, positive for sweepback

Symbol	Definition
$\mu_{bending}$	Approximation to generalized mass ratio for bending motion
$\mu_{generalized}$	Generalized mass ratio
$\mu_{torsion}$	Approximation to generalized mass ratio for torsional motion
ρ	Fluid density
σ	Local bending slope of elastic axis $\partial h/\partial y$
τ	Local rate of change of twist along elastic axis $\partial\theta/\partial y$
ω	Circular frequency of oscillation
ω_α	Circular frequency of first torsional vibration mode in air

SUBSCRIPTS

i	Subscript to indicate that the parameter is associated with ith strip station on strut
m	Subscript to indicate that the parameter is perpendicular to elastic axis

SUPERSCRIPT

$(\dot{})$	Dot over a quantity indicates differentiation with respect to time

ABSTRACT

A large body of experimental and theoretical flutter results for hydrofoil struts were analyzed to determine significant characteristics. Flutter was found to occur in two different structural mode shapes, corresponding to a predominantly bending mode and a predominantly torsional mode, respectively. The flutter mode shape was related to the vibration mode shapes and the generalized mass ratio of the strut at zero speed. The behavior of the hydroelastic modes of typical struts as a function of speed was investigated by using a strip theory with three-dimensional loading modifications. Flutter predictions for struts which underwent flutter in the torsional mode were usually conservative and predicted the correct mode shape. However, flutter predictions for struts which underwent flutter in the bending mode were unreliable in predicting the mode of flutter because of an extreme sensitivity to the loading modification used. Strut-foil systems of the inverted-T configuration typical of full-scale hydrofoil craft appear to undergo either bending flutter or torsional flutter, depending on pod and foil characteristics.

ADMINISTRATIVE INFORMATION

This work was authorized and funded under the Hydrofoil Development Program of the Naval Ship Systems Command, Subproject S4606, Task 1703. This report is a verbatim reproduction of a paper presented at the Ninth Symposium on Naval Hydrodynamics, 20-25 August 1972, Paris, France.

INTRODUCTION

The high speeds associated with many unconventional ships will require a better understanding of flutter and other hydroelastic phenomena than has been available for design of existing ships. Prominent among unconventional ships are hydrofoil craft and surface effect ships. Flutter is a recognized problem for the strut-foil systems of hydrofoil craft. The rudders contemplated for surface effect ships may be similarly vulnerable.

Much research has been done on the flutter of strut models analogous to the above systems. The initial demonstration of strut flutter was made

by Hillborne[1] in 1958. Further experimental work has often been accompanied by difficulties, including models that wouldn't flutter, models that were destroyed by flutter or divergence, and facility limitations. Numerous theoretical analyses have been produced, but none has been successful in predicting all experimental results conservatively.

Out of these efforts have come many clues to the nature of strut flutter. By combining previous results with some recent experimental and theoretical work, we have produced a concept of flutter involving two different flutter regions. This paper will discuss existing flutter data from the standpoint of two flutter regions and will present calculations which indicate the origin of the two regions. The expected accuracy of flutter speed predictions within each region will be described.

Existing data deal with a large number of simple struts and a small number of struts with tip pods, some with foils forming an inverted-T configuration. A sample configuration is shown in Figure 1. All tested configurations have been small-scale models. Most discussion will be devoted to simple struts and struts with pods. One strut with foils has been included.

All struts were cantilever supported from an effectively rigid foundation, so that the structural characteristics of the system were those of a cantilever beam in which both bending and twisting could occur. Because of the relatively high aspect ratio and thin profile of the struts, bending consisted of displacements perpendicular to the plane of the strut, while twisting occurred about a spanwise elastic axis. Vibration modes of the struts consisted of a series of modes which could usually be identified as predominantly bending or predominantly twisting or torsion.

The mode shapes of the struts at flutter inception could also be characterized as predominantly bending or torsion. In most cases, struts

---

[1]Hillborne, D. V., "The Hydroelastic Stability of Struts," Admiralty Res. Lab Report No. ARL/R1/G/HY/5/3 (1958). A complete listing of references is given on pages 53 and 54.

displayed either bending or torsional oscillations at flutter. This was the basis for dividing flutter phenomena into two regions. Flutter in one region occurred in a predominantly bending mode shape and will be referred to as bending flutter. Flutter in the other region occurred in a predominantly torsional mode shape and will be referred to as torsional flutter.

It appears that all hydrofoil struts, including those with pods and foils attached, undergo either bending flutter or torsional flutter. The type of flutter characteristic of a given strut can be determined by examining its vibration modes, except in a transition region where strong coupling of structural modes occurs. Most available data can be readily placed into the appropriate flutter regions.

Experimental results from each flutter region were examined separately. The two flutter regions corresponded to two ranges of generalized mass ratio. In the bending flutter region, struts had low values of generalized mass ratio, while struts in the torsional flutter region had high values of generalized mass ratio. Flutter speed varied differently in each region as a function of mass ratio or strut submergence, a related parameter.

Calculated flutter characteristics show substantial qualitative agreement with observed characteristics. Flutter was found to occur in a different hydroelastic mode in each flutter region. Predicted flutter inception speeds for torsional flutter were conservative for most struts, with many predictions being overconservative. Unfortunately, flutter speed predictions for bending flutter were not usable because two flutter modes were often predicted to be unstable in the bending flutter region, with the wrong mode predicted to be the least stable. This discrepancy was related to an extreme sensitivity of the flutter calculation to hydrodynamic loading modification in the bending flutter region.

EXPERIMENTAL FLUTTER CHARACTERISTICS

BENDING-TYPE AND TORSION-TYPE STRUTS

The flutter mode of a strut is strongly correlated with the nature of the vibration modes of the strut in air or in water. It is therefore convenient to define a method for classifying struts according to important differences in vibration modes. Strut mode shapes are those of a cantilever

beam, with bending displacements perpendicular to the plane of the strut and torsional rotations about a spanwise elastic axis. Mode shapes are designated by their similarity to the uncoupled mode shapes of a cantilever beam. Some uncoupled mode shapes are shown in Figure 2, numbered in order of increasing frequency.

All struts exhibit a fundamental (lowest frequency) vibration mode shape resembling first bending. Struts show a marked difference in their second modes, however, permitting struts to be divided into two groups. The second mode of any strut will consist of a second bending mode coupled with a first torsion mode, with one usually predominating. Predominance is determined by the relative linear displacements produced by bending and torsion, which provide an indication of nodal line characteristics. If the second vibration mode is predominantly second bending, the strut is a bending-type strut. If the second vibration mode is predominantly first torsion, the strut is a torsion-type strut.

Struts having little or no tip weighting are usually bending-type struts. Struts having relatively heavy pods are usually torsion-type struts. A transition region exists in which the second vibration mode of a strut is equally due to a second bending mode shape and a first torsion mode shape, with neither predominating. Struts in this transition region have moderately weighted pods or medium to large foils. The effect of foils in coupling second bending and first torsion is very pronounced when the foils are submerged due to the large rotary inertia effect at the tip of the strut. When such strong coupling occurs, it is impossible to classify the strut as bending type or torsion type.

In most cases the third vibration modes of bending-type struts are first torsion, while torsion-type struts have a third vibration mode resembling second bending. This observation indicates that a change in strut type usually involves a reversal in the order of the second and third mode shapes.

Most struts have the same mode order in air and in water. If there is a difference, the mode order in water should be used for classifying a strut. Either measurement or calculation can be used to determine the required mode shapes.

FLUTTER MODE SHAPES

The flutter mode shapes of bending-type struts are radically different from those of torsion-type struts. Bending-type struts undergo flutter in a predominantly first bending mode shape, while torsion-type struts undergo flutter in a predominantly first torsion mode shape. In accordance with the flutter mode shapes, flutter of bending-type hydrofoils will be referred to as bending flutter, and flutter of torsion-type hydrofoils will be referred to as torsional flutter.

The two types of flutter mode shapes have not been quantitatively measured, but were discovered because the very striking differences in mode shape were visually observed. Differences in flutter mode shapes were reported by Huang[2] as a result of flutter testing a strut with and without a heavy pod. The bending amplitude of the strut alone was reported to be considerably larger than the torsional amplitude which was also present. When the pod was added, the torsional amplitude became larger than bending.

A similar result was obtained in an experiment performed at the Naval Ship Research and Development Center (NSRDC) in which a bending-type strut and a torsion-type strut were flutter tested. Both struts had been previously tested but mode shapes were not reported. Motions of the struts were visually observed and recorded on video tape. The bending-type strut, Model A of Reference 3, underwent large first bending oscillations with little evident twisting. In contrast, the torsion-type strut, Model 2T of Reference 4, displayed first torsion oscillations with no visible bending.

---

[2]Huang, T. T., "Experimental Study of a Low Modulus Flutter Model for Strut-Foil-Pod Configurations," Hydronautics, Inc. Technical Report 459-2 (Jul 1967).

[3]Squires, C. E., Jr., "Hydrofoil Flutter, Small Sweep Angle Investigation - Final Report," Grumman Aircraft Engineering Corporation Report DA Nonr-3989.3 (Nov 1963).

[4]Baird, E. F. et al., "Investigation of Hydrofoil Flutter - Final Report," Grumman Aircraft Engineering Corporation Report DA 10-480-3 (Feb 1962).

In addition to a change in mode shape, a change in frequency would be expected when the flutter mode changes. Several pod configurations for Model 2T were flutter tested,[4] and a significant change in flutter frequency occurred when the strut changed from bending-type to torsion-type. Flutter data for this strut are plotted in Figure 3. As the pod mass was increased and the pod center of gravity was moved aft, an abrupt increase in frequency occurred between pod configurations A and B. Vibration modes calculated in water identify pod configuration A as a bending-type model, while pod configuration B gives strongly coupled second bending and first torsion modes for both its second and third modes and therefore falls in the transition region between bending-type and torsion-type struts. Pod configuration C was a torsion-type strut.

Although mode shapes have been observed in only a small number of cases, other aspects of flutter data exhibit a dual nature corresponding to differences in mode shape. The effects of generalized mass ratio and of strut submergence vary according to the flutter region. These effects will be discussed below.

GENERALIZED MASS RATIO

Generalized mass ratio is a parameter which indicates the relative importance of structural and fluid inertia in determining the motion of a strut. Both structural and fluid inertia are related to the vibration mode shape (and therefore to the elastic properties) of the strut. This relationship is included in the most general form of the parameter, which can be expressed in terms of matrix elements as

$$\mu_{generalized} = \frac{\begin{Bmatrix} H_i \\ \Theta_i \end{Bmatrix}^T [M] \begin{Bmatrix} H_i \\ \Theta_i \end{Bmatrix}}{\begin{Bmatrix} H_i \\ \Theta_i \end{Bmatrix}^T [M^*] \begin{Bmatrix} H_i \\ \Theta_i \end{Bmatrix}}$$

This expression reduces to the mass ratio traditionally used in flutter analysis when pure bending motion of uniform amplitude is assumed. A similar simplification occurs when pure torsional motion is assumed. These assumed

motions provide suitable approximations to the mode shapes of bending and torsional flutter. Exact flutter mode shapes are of course not available. Therefore simplified expressions for mass ratio were used in analyzing experimental flutter results.

It was found that bending flutter occurs at low values of mass ratio and that torsional flutter occurs at high values of mass ratio. Other than this generalization, comparisons involving mass ratio will not be made between struts having different flutter modes. Such comparisons would require extensive calculations involving exact flutter mode shapes, which are not available. Calculations presented later indicate that bending flutter and torsional flutter involve entirely different vibration modes and do not represent different mass ratio ranges of the same mode. Mass ratio will be used as a parameter for comparing flutter results of similar mode. Each flutter region will be discussed separately.

Bending Flutter Region

In the bending flutter region, generalized mass ratio can be approximated by dividing total strut mass by the mass of a cylinder of water circumscribing the strut. The cylinder of water should have a diameter equal to the strut chord and a length equal to the submerged span of the strut. This cylinder of water approximates the added mass of the strut for the first bending mode shape associated with bending flutter. Bending mass ratio may be written symbolically as

$$\mu_{bending} = \frac{mL}{\pi \rho b^2 \ell}$$

Flutter speeds obtained from bending-type struts are plotted as a function of bending mass ratio in Figure 4. Values of bending mass ratio range from 0.1 to 0.66. The flutter speeds fall into two groups. The higher flutter speeds correspond to strut models which are geometrically larger by a factor of approximately 4 than strut models represented in the lower group. Within each group, the flutter speeds are sensitive to mass

ratio and a sweep parameter κ. The sweep parameter[5,6] combines sweep angle and unswept aspect ratio into a single parameter. Numerical values of κ are given for the data points in Figure 4. For similar size models, the data can be fairly consistently divided into families based on similar values of κ as shown. An increase in sweep angle therefore increases the flutter speed, while an increase in aspect ratio decreases the flutter speed. Lines of constant κ value approach zero as mass ratio decreases in a manner which could be approximated by a square root dependence on mass ratio, a relation which has previously been observed[3] for low mass ratio struts. Similar trends have been predicted in the lower mass ratio region when sweep angle was included in the analysis.[6,7,8] Groups of different sized models can be correlated by dimensional analysis. It has been shown[9] that the flutter speeds are related according to the square root of bending or torsional stiffness.

Torsional Flutter Region

Generalized mass ratio for torsional motion can be represented by the ratio of the total moment of inertia of a strut and the added moment

---

[5]Jordan, P. F., "On the Flutter of Swept Wings," Journal of the Aeronautical Sciences, Vol. 24, No. 3, pp. 203-210 (1957).

[6]Caporali, R. L. and E. J. Brunelle, "Hydrofoil Instability at Low Mass Density Ratios," Princeton University Aerospace and Mechanical Sciences Report No. 670 (Mar 1964).

[7]Herr, R. W., "A Study of Flutter at Low Mass Ratio with Possible Application to Hydrofoils," NASA TN-D-831 (May 1961).

[8]Squires, C. E., Jr. and E. F. Baird, "The Flutter Characteristics of a Hydrofoil Strut," Proceedings of the Fourth Symposium on Naval Hydrodynamics, pp. 739-759 (1962).

[9]Ho, H. W., "The Development and Testing of Low Modulus Flutter Models of a Base-Vented Strut," Hydronautics, Inc. Technical Report No. 459-1 (May 1965).

of inertia of the submerged portion of the strut. In the present work, rotation was assumed to occur about the elastic axis of the strut. The resulting torsional mass ratio may be written

$$\mu_{torsion} = \frac{I_\alpha}{\pi\rho b^4 (1/8 + a^2)\ell + I^*_{\alpha,\,pod}}$$

Available flutter speeds for torsion-type struts are plotted as a function of torsional mass ratio in Figure 5.[2,4,10,11] A substantial amount of data is shown which was obtained at NSRDC and has not been previously published. All strut models in this group had pods and were similar in size to the struts described in Reference 4. A complete description of these data will be published in the near future.

As shown in Figure 5, torsional flutter has been obtained at values of torsional mass ratio between 0.61 and 6.2. Flutter speeds generally decrease as mass ratio increases. The wide variation in flutter speed results at least in part from wide variation in strut characteristics. In an attempt to adjust flutter speeds for differences in geometric size and torsional frequency, the data have been replotted in Figure 6 after normalization by the factor $b\omega_\alpha$. This normalization was successful for values of mass ratio between 2.0 and 6.2, but large variations still exist at values below 2.0. Parameters that differ among the lower mass ratio models include the elastic axis location, profile, sweep angle, and submergence of the struts, and the size and inertial characteristics of pods attached to the struts. The effects of strut profile have recently been investigated at NSRDC, and results for three different profiles are indicated in Figure 6. At speeds high enough to produce ventilation over the entire chord of the strut, a ventilated cavity originating from a blunt

---

[10]Abramson, H. N. and G. E. Ransleben, Jr., "An Experimental Investigation of Flutter of a Fully Submerged Subcavitating Hydrofoil," Journal of Aircraft, Vol. 2, No. 5, pp. 439-442 (1965).

[11]Besch, P. K. and Y. N. Liu, "Flutter and Divergence Characteristics of Four Low Mass Ratio Hydrofoils," Naval Ship Research and Development Center Report 3410 (Oct 1970).

leading edge on a strut substantially destabilizes the system. The effects of strut submergence will be discussed later.

The reduced flutter speeds for torsional flutter exhibit the characteristics found in classical hydrofoil flutter. The flutter speed parameter gradually decreases to a minimum value as mass ratio decreases, and then increases rapidly for related series of strut models at lower values of mass ratio. Minimum values occur approximately between mass ratios of 2.0 to 3.0. The effect of mass ratio on torsional flutter speeds is similar to that predicted by classical two-dimensional flutter theory and also to that predicted in the higher mass ratio region in finite sweep angle analyses.[6,7,8]

STRUT SUBMERGENCE

The effects of strut submergence on flutter speed are closely related to the effects of generalized mass ratio. When the simplified forms of mass ratio are used, the two parameters are inversely proportional to one another. The close relationship is evident in experimental flutter results in which submergence has been varied without changing other strut characteristics. These results, shown in Figure 7, constitute a replotting of data contained in Figures 4 through 6 but are given to illustrate the effects of submergence directly.

Flutter speeds for bending-type struts decrease as strut submergence increases, with minimum flutter speeds occurring at full submergence. The increase in submerged length produces a decrease in mass ratio and therefore a decrease in flutter speed. Torsion-type struts show a local minimum in flutter speed at approximately 50-percent submergence. This local minimum would be expected to occur if the strut configuration passed through intermediate values of mass ratio, and will not necessarily correspond to 50-percent submergence. An increase in flutter speed will of course occur as the submergence becomes very small regardless of the mass ratio. The effect of submergence on the strut model with pod and foils is similar to that observed for struts without foils in the bending flutter region and at high values of mass ratio in the torsional flutter region.

Strut submergence also affects the vibration mode shapes of struts and has a particularly large effect on the second bending mode. As a

result, a strut could change from a bending-type strut to a torsion-type strut during changes in submergence. Because of the occurrence of minimum flutter speeds at different depths for different modes and the possibility of different flutter modes occurring at different depths, it is conceivable that a strut could undergo bending flutter at one depth and torsional flutter at another depth.

THEORETICAL FLUTTER CHARACTERISTICS

The dual nature of experimental flutter results also appears in theoretical results. Bending flutter and torsional flutter correspond to instabilities in different hydroelastic modes. Transition from bending flutter to torsional flutter occurs when the torsional flutter mode becomes less stable than the bending flutter mode.

The frequency and mode shape characteristics of the hydroelastic modes involved in flutter are predicted accurately in the flutter analysis. However, damping characteristics and, consequently, flutter speeds are not predicted accurately. In the bending flutter region, flutter speed predictions are not usable because a second mode is also predicted to be unstable which does not correspond to experimental results. Flutter speed predictions in the torsional flutter region correctly indicate the unstable mode but are generally overconservative. Calculated hydroelastic modes of a strut with attached foils indicate that the strut underwent torsional flutter at a speed which was overconservatively predicted.

FLUTTER THEORY

Understanding the differences between bending flutter and torsional flutter requires consideration of the behavior of the hydroelastic modes,[12] or resonances, of the strut systems over a wide range of speeds, and not merely a calculation of each strut's speed of neutral stability. This

---

[12] Bisplinghoff, R. L. and H. Ashley, "Principles of Aeroelasticity," John Wiley and Sons, Inc., New York (1962), p. 235.

approach was in fact used in a paper[8] presented at the Fourth Symposium on Naval Hydrodynamics. This earlier paper described the hydroelastic modes of bending-type struts only. The present paper extends the earlier results to include a description of the hydroelastic modes of torsion-type struts as well.

Hydroelastic modes are the vibration modes of the strut-fluid system and correspond to eigenvalues and eigenvectors of the velocity-dependent equations of motion. The equations of motion were generated by assuming a lumped parameter representation for the strut, with elastic and inertial properties lumped at discrete points along a straight elastic axis. This procedure is well established as an accurate means of predicting vibration mode shapes and frequencies of elongated structures in air. The hydrodynamic forces on the strut were also lumped at stations along the axis. Values of structural parameters and hydrodynamic forces at spanwise stations were assigned by dividing the strut into strips normal to the elastic axis. A numerically converged solution was obtained when 10 strips were used.

Displacements were assumed to occur in bending normal to the plane of the strut and in torsion about the strut elastic axis. The equations of motion for the entire system written in matrix form are

$$[M] \begin{Bmatrix} \ddot{h}_i \\ \ddot{\theta}_i \end{Bmatrix} + [C] \begin{Bmatrix} \dot{h}_i \\ \dot{\theta}_i \end{Bmatrix} + (1 + jg)\,[K] \begin{Bmatrix} h_i \\ \theta_i \end{Bmatrix} = \{F_i\}$$

The hydrodynamic force F was expressed in terms of the physical displacements and their time derivatives, permitting the structural and hydrodynamic expressions to be combined. Further simplication is achieved by representing strut motion as a series of standing waves in the form

$$h_i = H_i\, e^{st} \qquad \text{and} \qquad \theta_i = \Theta_i\, e^{st}$$

The resulting system of linear equations for the hydroelastic system is

$$(s^2[M'] + s[C'] + [K']) \begin{Bmatrix} H_i \\ \Theta_i \end{Bmatrix} = \{0\}$$

Solutions to the above equations are the complex eigenvalues of s, which may be written

$$s = -\zeta\omega \pm j\sqrt{1-\zeta^2}\,\omega$$

in terms of the damping ratio ζ and the undamped natural frequency ω. Each eigenvalue of s corresponds to a mode of oscillation of the strut-fluid system. Flutter occurs at the lowest speed for which the real part of one of the eigenvalues becomes zero.

Eigenvalues for selected speeds were obtained by a digital computer calculation based on Muller's quadratic method.[13] Flutter speeds were determined by interpolation among damping values across the zero damping axis. Eigenvectors were also obtained, giving the vibration mode shapes in standing-wave form.

The most general form of strut motion is composed of traveling waves as well as standing waves. Further calculations were therefore made to determine whether traveling-wave oscillations were occurring. Traveling waves were found in connection with bending motion and will be described later.

HYDRODYNAMIC LOADING

Hydrodynamic loading on discrete sections of the strut was calculated with a strip theory. The theory was formulated to allow spanwise variation of the loading so that the effects of three-dimensional flow could be investigated.

The lift and moment expressions used were

$$-P_i = p_i \pi \rho b_i^2 \left[\ddot{h}_i - V_n\dot{\theta}_i + V_n\dot{\sigma}_i \tan\Lambda_{ea} + b_i a_i\left(\ddot{\theta}_i + V_n\dot{\tau}_i \tan\Lambda_{ea}\right)\right]$$

$$- C_{\ell_{\alpha,i}} \rho V_n b_i\, C(k)\, w_1$$

---

[13] Wilkinson, J. H., "The Algebraic Eigenvalue Problem," Oxford University Press, New York (1965).

$$-M_i = p_i \pi \rho b_i^4 (1/8 + a_i^2)(\ddot{\theta}_i + V_n \dot{\tau}_i \tan \Lambda_{ea}) + p_i \pi \rho b_i^2 V_n (\dot{h}_i + V_n \sigma_i \tan \Lambda_{ea})$$

$$+ p_i \pi \rho b_i^3 a_i (\ddot{h}_i + V_n \dot{\sigma}_i \tan \Lambda_{ea}) - p_i \pi \rho b_i^2 V_n^2 (\theta_i - a_i b_i \tau_i \tan \Lambda_{ea})$$

$$+ 2\pi \rho V_n b_i^2 \left[\frac{1}{2} p_i (a_i - a_{c,i}) \frac{C(k) \cdot C_{\ell_{\alpha,i}}}{2\pi} \right] w_i$$

where

$$w_i = -\dot{h}_i + V_n \theta_i - V_n \sigma_i \tan \Lambda_{ea} + b_i \left(\frac{C_{\ell_{\alpha,i}}}{2\pi} + a_{c,i} - a_i \right) (\dot{\theta}_i + V_n \tau_i \tan \Lambda_{ea})$$

In this formulation, spanwise loading variations were introduced separately for circulatory and noncirculatory loading. The loading due to circulatory flow was varied by inserting steady values of lift slope $C_{\ell\alpha}$ and aerodynamic center a_c obtained by a separate calculation. This approach was originated by Yates.[14] The noncirculatory terms were varied by inclusion of a multiplicative factor p. The factor permitted reducing the magnitude of the noncirculatory loading below that associated with two-dimensional flow. This modification was introduced by the authors,[15] in accordance with a suggestion by Yates.[16] Spanwise distributions for p will be discussed later.

---

[14] Yates, E. C., Jr., "Calculation of Flutter Characteristics for Finite-Span Swept or Unswept Wings at Subsonic and Supersonic Speeds by a Modified Strip Analysis," NACA RM L57L10 (1958).

[15] Liu, Y. N. and P. K. Besch, "Hydrofoil Flutter Analysis, Using a Modified Strip Theory," Naval Ship Research and Development Center Report 3624 (Jul 1971).

[16] Yates, E. C., Jr., "Flutter Prediction at Low Mass-Density Ratios with Application to the Finite-Span Noncavitating Hydrofoil," AIAA Third Marine Systems and ASW Meeting (Apr-May 1968).

The given expressions correspond to two-dimensional hydrodynamic loading when a lift slope of 2π, an aerodynamic center location at quarter chord, and a noncirculatory modification factor of unity are used. Three-dimensional loading requires that appropriate spanwise distributions of these quantities be used. In a number of flutter calculations presented later, the effects of three-dimensional flow were studied by varying the above quantities but keeping all spanwise values equal.

Spanwise distributions of lift slope and aerodynamic center were obtained from lifting surface theory.[17] The distributions were calculated by using a uniform angle of attack along the span of the strut and an antisymmetric loading boundary condition at the free surface.

Two different distributions of noncirculatory modification factor were used, one for low frequencies and one for high frequencies.[15] At low frequencies, the factor consisted of the three-dimensional added mass of the strut, expressed as a fraction of the two-dimensional added mass, outboard of the spanwise position being considered. The free surface was treated as a reflecting plane. At high frequencies, the spanwise distribution of added mass on a surface-piercing strut decreases to zero at the free surface. This condition was approximated by assuming the midspan of the submerged portion of the strut to be a reflecting plane and using the low frequency distribution on either side.

Values of the nondimensional frequency, $\ell\omega^2/g$, were used to distinguish between low frequency and high frequency conditions, indicating that the generation of gravity waves was involved in the boundary condition. The low frequency condition exists for values of $\ell\omega^2/g$ of 1 or less, while high frequency loading corresponds to values of $\ell\omega^2/g$ of 10 or greater.

BENDING FLUTTER

The hydroelastic modes of several bending-type struts were calculated. In general, two unstable modes were predicted for each strut. One of the

---

[17] Ashley, H. et al., "New Directions in Lifting Surface Theory," AIAA Journal, Vol. 3, No. 1, pp. 3-16 (1965).

unstable modes showed fair correlation with experimental flutter occurrences, while the second unstable mode did not correlate well with experimental results. It therefore appears that one unstable mode corresponded to the experimentally observed instabilities for all of the struts, while the other unstable mode was incorrectly predicted to be unstable. The incorrect prediction was, in fact, found to occur only for limited ranges of spanwise loading inputs, suggesting that the prediction was caused by a slightly inaccurate loading formulation in a highly sensitive calculation.

The mode in which bending flutter occurred had a first bending mode shape and had the lowest frequency among the existing modes at the experimental flutter speed. At speeds below flutter, the mode was highly damped. Its damping decreased rapidly in a short speed interval prior to flutter. Values of damping were predicted nonconservatively.

These results will be illustrated by presenting detailed characteristics of the hydroelastic modes of a typical bending-type strut, Model 2 of Reference 4. The structural characteristics and three-dimensional loading parameters for Model 2 are given in the Appendix. Several hydroelastic modes calculated for Model 2 are shown as functions of speed in Figures 8 and 9. The damping ratio ζ was plotted without structural damping because no experimental values were available. Predominant mode shapes are indicated on the frequency curves. Predicted instabilities must be compared with an experimental flutter speed of 81 knots and a frequency of 4.1 Hz at that speed. The mode shape at flutter was observed to be predominantly first bending in a motion picture of the experiment.

Flutter is predicted to occur at 83 knots in the presence of two-dimensional loading, as shown in Figure 8. The instability occurs in a mode which first appears, fully damped, at a speed of 30 knots and decreases in stability as speed increases until neutral stability is reached at 83 knots. Although the unstable mode appears at a speed near that at which mode 1 damps out, the two modes coexist over a small speed range. Therefore the unstable mode is considered to be a new mode rather than mode 1. The frequency and mode shape of the new mode show good agreement with experiment. Mode 3 is stable and increases in frequency as speed increases.

The predicted instabilities are much different, and less accurate, when three-dimensional loading modifications are included. Despite the

theoretically improved loading expression, the flutter speed predicted for the new mode is a highly nonconservative 147 knots. Mode 3 is unstable over the entire speed range, except at low speeds where inclusion of structural damping would produce a positive damping ratio. Both unstable modes have a first bending mode shape in the vicinity of the experimental flutter speed. The frequency of mode 3 now decreases rapidly with speed, but nevertheless does not decrease sufficiently to agree with experiment at 81 knots. On the other hand, the frequency of the new mode shows fairly good agreement with experiment at 81 knots. In this case and in general, frequencies of hydroelastic modes are predicted more accurately than damping characteristics, and are less sensitive to variation in hydrodynamic loading. It is concluded that flutter occurred experimentally in the new mode, and that mode 3 is not unstable below 81 knots.

Each of the loading modification parameters was varied independently to determine its effect on predicted flutter instabilities. Equal loading was used at all spanwise positions. The resulting flutter speeds for the new mode and mode 3 are shown in Figure 10. Mode 3 becomes unstable when any of the three modification parameters is changed sufficiently from two-dimensional values. A three-dimensional value of lift slope produces greater instability in mode 3 than three-dimensional values of the other parameters. Interactions among parameters and variations in strut configuration also affect the stability of mode 3. The behavior of hydroelastic modes 1 and 2 was not significantly affected by the variation of applied loading.

The nature of the oscillations experienced by Model 2 at flutter was further investigated in order to determine whether the oscillations consisted of standing or traveling waves. Calculations by Dugundji et al.[18] and Prasad et al.[19] had indicated a bending flutter condition occurring in the form of traveling waves for low mass ratio wings. The present complex

---

[18]Dugundji, J. and N. Ghareeb, "Pure Bending Flutter of a Swept Wing in a High-Density, Low-Speed Flow," AIAA Journal, Vol. 3, No. 6, pp. 1126-1133 (1965).

[19]Prasad, S. N. et al., "Bending-Torsional Flutter of a Swept Wing in a High-Density, Low-Speed Flow," AIAA Journal, Vol. 5, No. 2, pp. 316-321 (1967).

eigenvalue calculation restricted oscillations to a series of standing waves in which nodal lines remained stationary and all displacements in each mode maintained their relative distributions at all times. Traveling waves are characterized by nodal lines which traverse the entire surface of the strut during a cycle of oscillation.

A direct solution to the equations of motion was attempted by using a finite difference technique in the time domain.[20] The method of solution yields a time history of the transient motion following an initial excitation of finite duration. Flutter inception occurs when oscillations change from decreasing to increasing amplitude. Neutral stability should occur at the same speed using either method of solution. Calculations were performed by a digital computer program which required that hydrodynamic force expressions be real. Because of this restriction, the imaginary part of the Theodorsen circulation function was omitted from the loading used.

Unsatisfactory results were obtained from the direct method of solution. The predicted flutter speed did not agree with that predicted by the eigenvalue calculation. Furthermore, values of negative damping above flutter inception were so large that no oscillation occurred. As a result, the presence of traveling waves could not be detected. The discrepancies between the two methods of solution may have resulted from the difference in hydrodynamic loading used. It is evident that further investigation of this method of calculation is required.

The hydroelastic mode characteristics of Model 2 are typical of three other bending-type struts that were analyzed. Flutter predictions using two-dimensional loading were often fairly accurate. The mode 3 instability appeared in two of the three additional calculations using three-dimensional loading. The flutter inception speeds for the new mode were again nonconservative, and less accurate than those obtained using two-dimensional loading. Frequencies predicted for the new mode agreed well with frequencies observed at flutter, while those for mode 3 did not

---

[20] Peterson, L., "Theoretical Basis for SADSAM Computer Program," MacNeal-Schwendler Corporation Project Report (Dec 1970).

agree well. Frequency predictions were equally accurate for both types of loading. Predicted mode shapes for the new mode were predominantly first bending. This agrees with mode shapes observed for bending flutter.

The damping behavior of the new mode as a function of speed shows qualitative agreement with experimental results. In an experiment performed at NSRDC, damping was found to be extremely high for a bending-type strut at all speeds below flutter inception. At flutter inception, damping decreased sufficiently to permit flow-excited oscillations of large amplitude. This behavior would be expected of an instability occurring in the new mode, which decreases in damping from a highly damped condition at intermediate speeds.

In view of the more accurate frequency correlations of the new mode and its high damping characteristics at intermediate speeds, it is concluded that bending flutter occurs in the mode designated as the new mode. Measurements of damping of strut modes at various speeds are needed to confirm this conclusion. The appearance of a calculated instability in mode 3 is probably caused by extreme sensitivity of the calculated damping to load variation. The present flutter calculation can be used to indicate a possible occurrence of bending flutter, but cannot be used for estimating flutter speeds. Design calculations should be performed with both two-dimensional and three-dimensional loading so that all potential instabilities will be discovered.

TORSIONAL FLUTTER

The calculated hydroelastic modes of torsion-type struts exhibit more simple behavior than those of bending-type struts. Only one mode is unstable. It is the mode with the second-lowest frequency, and therefore with a predominantly first torsion mode shape, at zero speed. Low damping is predicted in this mode at all speeds below flutter, in contrast to the high damping predicted in the bending flutter mode. Observed characteristics of torsional flutter correlate well with the characteristics of this hydroelastic mode. A mode analogous to the new mode previously described appears for some torsion-type struts, but it is stable throughout the speed range of interest. Three-dimensional loading modifications have very little

effect on the qualitative characteristics of the hydroelastic modes of torsion-type struts, but do change the predicted flutter speeds.

Predicted torsional flutter speeds ranged from 59 percent conservative to 36 percent nonconservative when three-dimensional loading was used. The predicted flutter speeds were nonconservative for struts with extremely heavy pods, and became increasingly conservative as the struts decreased in mass ratio and approached the bending flutter region.

As an example of hydroelastic modes for torsion-type struts, the modes for Model 2T of Reference 4 are shown in Figure 11. The structural characteristics of Model 2T are identical to those of Model 2 except for the addition of a long, slender pod to the strut tip. The pod is described in the Appendix. The damping ratio includes the value of structural damping measured at zero speed. One value of damping ratio and frequency was reported in Reference 4, and the others were measured at NSRDC by deflecting the strut with an attached line and cutting it during the test runs. A flutter speed of 18.1 knots was obtained at NSRDC, and a frequency of 6.4 Hz was observed at that speed. The vibration mode shape prior to and at flutter was predominantly first torsion.

Flutter is predicted to occur in mode 2 at 14.1 knots when two-dimensional loading is used. This prediction is conservative by 22 percent. The calculated damping values are lower than the experimental values, but show a similar variation with speed. Frequencies of the hydroelastic modes remain relatively constant as a function of speed, and agree well with available data. The mode shape of the unstable mode, mode 2, changes from first torsion to first bending prior to the predicted flutter inception, so that flutter is incorrectly predicted to occur with a first bending mode shape.

Slight changes occur in the hydroelastic modes when three-dimensional loading modifications are included. The three-dimensional loading used for Model 2 was also used for Model 2T. The damping of mode 2 increases, remaining below the experimental values for part of the speed range below flutter inception but yielding a flutter speed of 18.8 knots, which is very close to the experimental value but is slightly nonconservative. The flutter mode shape is predicted to be predominantly first torsion, which is the mode shape that was observed.

The good agreement between experimental and theoretical characteristics of mode 2 clearly establishes that the instability has been correctly predicted. Identification of the unstable mode is easier than for Model 2 because sufficient data are available and the modes are unambiguous in predicting instability.

The effects of independent variation of the loading modification parameters on predicted flutter speeds for Model 2T are shown in Figure 12. Equal values of loading were used at all spanwise stations. The calculation is conservative and reasonably accurate using two-dimensional loading, and is unaffected by loading modifications except when lift slope is reduced below 70 percent of the two-dimensional value. While the calculation is sensitive only to lift slope for the conditions shown, strong interactions occur among the modifying parameters when they are varied simultaneously. This interaction is demonstrated by the 18.8 knot flutter speed prediction obtained when three-dimensional values are used for all modifying parameters.

No mode corresponding to the new mode described for Model 2 appears in the speed range shown for Model 2T. Such a mode does appear at higher speeds, however, but remains stable at all speeds for which calculations were made.

An indication of traveling wave motion was found in the flutter mode of Model 2T. However, a discrepancy in calculated flutter speed similar to that found for Model 2 prevents full confidence in the results. The direct method of calculation yielded increasing and decreasing oscillations above and below a different flutter speed from that obtained by eigenvalue calculation. Calculated mode shapes in bending and torsion at flutter are shown in Figure 13 as functions of time. The bending oscillations are traveling waves, while the torsional oscillations are standing waves. Strut deflections due to torsion were approximately twice as large as those due to bending. Therefore the flutter oscillations were predominantly standing waves, although traveling waves were not insignificant.

Flutter characteristics calculated for several other torsion-type struts using three-dimensional loading were similar to those of Model 2T. Flutter invariably occurred in mode 2. Calculated flutter speeds, which are compared with experimental values in Figure 14, ranged from 59 percent conservative for very light pods to 36 percent nonconservative for very

heavy pods. Frequency predictions showed good agreement with measured values at the experimental flutter speeds. Flutter mode shapes were predicted to be first torsion, with occasionally significant amounts of first bending or second bending. These mode shape predictions agree with visually observed mode shapes.

Examples of predicted flutter characteristics of both bending-type and torsion-type struts, as well as a strut in the transition region (pod configuration B), are shown in Figure 3. The increasingly conservative torsional flutter speed predictions are evident as pod inertia decreases, until bending flutter occurs with pod configuration A. In view of the good correlation between theoretical and experimental frequency and mode shape in the torsional flutter region, it is concluded that torsional flutter is an instability of hydroelastic mode 2 for torsion-type struts.

A new mode similar to that of Model 2 and Model 2T also appears in the hydroelastic modes of other torsion-type struts. This mode appears at lower speeds for struts with lighter pods. The stability of the new mode decreases as strut pods become lighter and strut configurations shift from torsion type to bending type. Bending flutter appears to originate when the new mode becomes unstable at a lower speed than the mode which is unstable in torsional flutter. A shift in the mode shapes of the second and third modes occurs as part of this transition. It is perhaps not coincidental that the mode which is unstable in the torsional region and the mode which is incorrectly predicted to be unstable in the bending region both originate as first torsion modes.

Calculations made for struts with large pods included an approximate correction for hydrodynamic forces acting on the pod. The correction, added to the tip of the strut, consisted of the linearized lift and moment due to the unsteady motion of a pod-sized slender body, and is described on page 417 of Reference 12. This correction produced much lower flutter speeds than using pod virtual mass alone, particularly for heavy pods.

STRUTS WITH FOILS

Successful flutter analysis of strut-foil systems is of considerable practical importance because struts will generally be used in combination with load-bearing foils. Only inverted-T strut-foil configurations have

been considered in the present work, in view of the interest of the U. S. Navy in such configurations. It is clear that for such systems foils have a sizable effect on flutter characteristics. Flutter speeds obtained experimentally by Huang[2] showed an increase of as much as 146 percent when a pod was replaced by a pod and foil combination of equal mass. The parameters governing the effects of foils on flutter characteristics have only begun to be investigated. An early discovery has been that foil angle of attack is an important flutter parameter.[2]

While experimental results are relatively scarce, much can be deduced about the flutter characteristics of struts with foils by considering the structural effects of adding foils. A strut with no tip attachment will usually be a bending-type strut, and a heavily tip-weighted strut will be a torsion-type strut. Therefore struts with foils will vary from bending type to torsion type, with many configurations being in the transition region, according to the size and weight of the foils. Other parameters will be important to the extent that they produce bending-type or torsion-type characteristics. The rotational inertia of the foils will affect the coupling between the second and third vibration modes, so that large or high aspect ratio foils will produce struts in the transition region. Large or heavy pods tend to produce torsion-type struts. These effects are related to the generalized mass ratio of the strut.

Flutter characteristics calculated for a strut with foils were consistent with these deductions. The strut had a large pod and full-sized foils. The calculated instability occurred in hydroelastic mode 2, the unstable mode in torsional flutter. The flutter speed prediction was overconservative. The second and third vibration modes at zero speeds were composed equally of second bending and first torsion mode shapes, indicating that the strut was in the transition region.

The flutter analysis performed on the strut-foil model[2] will be described in detail to permit comparison with previous results. Structural characteristics of the model are given in the Appendix. Several approximations were made in obtaining a theoretical representation for the pod and foils. Structural properties of the pod and the foils were represented by adding equivalent masses and moments of inertia to the tip of the strut.

Hydrodynamic loading on the pod and foils was represented only by adding their added mass and moment of inertia to the structural components.

The effects of the pod and foils on the vibration mode shapes of the submerged strut are shown in Figure 15. It was necessary to use 67 percent of the published values for bending and torsional stiffness to achieve agreement with measured in-air frequencies. These stiffness values were used for in-water frequency calculations and hydroelastic mode calculations as well. The strut alone is a bending-type strut, and the strut with pod is a torsion-type strut. The second and third modes of the strut with pod and foils each exhibit both first torsion and second bending oscillations. Strong couplings due to the foils has also produced similar frequencies for these modes. The strut-foil model must be classified in the transition region. The effect of the foils is particularly striking because the pod-foil combination has the same mass as the pod used on the strut-pod model.

Flutter was found experimentally to depend on the angle of attack of the foil. Two flutter conditions were obtained: at 16.6 knots with an angle of attack of -4 deg, and at 18.1 knots with an angle of attack of -2 deg. Testing was halted prior to flutter at higher angles of attack because divergent deflections of the strut began to occur. Flutter mode shapes were described as equally large bending and torsional deflections. The bending deflections were seen to change from second bending to first bending, while the torsional deflections were consistently first torsion. Structural damping was not determined experimentally.

Calculated hydroelastic modes for the strut-foil model are shown in Figures 16 and 17. Both two-dimensional and three-dimensional loading yield a flutter instability in mode 2. The predicted flutter speed is overconservative at approximately 6 knots in both cases. An additional unstable mode is found which is different for the two types of loading. Two-dimensional loading yields an instability in the new mode, while three-dimensional loading yields an instability in mode 3. The frequencies predicted by using three-dimensional loading for mode 2 at the observed flutter speeds agree well with the experimental frequencies, while those predicted for mode 3 do not agree well. On the basis of the usually reliable frequency calculation of three-dimensional loading, it is concluded

that flutter occurred experimentally in mode 2. Additional damping data for individual modes are needed to confirm this conclusion.

Predicted mode shapes do not agree with observations. Mode 2 consisted of both second bending and first torsion oscillations at low speeds, but showed almost exclusively first bending oscillations at the experimental flutter speed.

Experimental[2] and theoretical results were also obtained by the strut with a pod lighter than, and equal to, the weight of the pod with foils. Torsional flutter occurred in both cases, at 20.1 knots with the smaller pod weight and at 9.5 knots with the larger pod weight. The large decrease in flutter speed when weight was added to the pod would be expected at low values of torsional mass ratio, as may be seen in Figure 5. Converting part of the pod mass into foils has raised the flutter speed, and has had a similar effect to reducing the pod mass. The foils have reduced the generalized mass ratio of the strut. Calculations of generalized mass ratio are required in order to correlate experimental results with values of this parameter.

It is apparent that additional experimental and theoretical research is needed to adequately understand flutter of struts with foils. Experimental results can provide a reliable indication of the effects of foil-related parameters and can lead to accurate simulation of full-scale systems with reduced-scale models. Theoretical research is needed to improve the accuracy of flutter speed predictions.

DISCUSSION

The primary deficiency of the present flutter analysis is its prediction of damping. This deficiency results in inaccurate predictions of flutter speed for most struts. In the torsional flutter region, the inaccuracy is strongly correlated with the value of torsional mass ratio of the strut. The relationship between experimental and theoretical flutter speeds has been illustrated in Figure 14. Predictions follow a fairly well-defined curve which is overconservative at low mass ratio, quite nonconservative at high mass ratio, and which crosses over experimental values at a mass ratio of slightly less than 2. It should be noted that the single very nonconservative prediction was strongly influenced by

the presence of a large pod, and is therefore not strictly representative of flutter characteristics of simple struts.

The conservative predictions obtained at low values of torsional mass ratio are highly significant. Many previous studies of hydrofoil and airfoil flutter have shown a tendency for predicted flutter speeds to become nonconservative at low values of mass ratio, leading to a loss of confidence in flutter predictions in this region. These studies have used two-dimensional loading without accounting for sweep angle. The present analysis, and a similar analysis[4] made previously, showed no tendency for predictions to become nonconservative at low mass ratio for torsional flutter. It appears that the most significant difference in the two types of calculations is the inclusion of sweep angle as a parameter which couples structural and hydrodynamic effects. The present calculation should reliably indicate the presence of a flutter instability throughout the mass ratio range shown in Figure 14. Additional comparisons with existing flutter data can help to determine the accuracy of flutter speed prediction to be expected as a function of mass ratio.

Improvement in the accuracy of flutter speed prediction will require improvement in the hydrodynamic loading formulation. The sensitivity of calculated damping to small changes in loading, particularly for bending-type struts, suggests that hydrodynamic loading must be very accurately described in order to obtain accurate flutter speed predictions. Possible sources of inaccuracy in the loading formulation are the presence of cavitation, real fluid effects involving the boundary layer and wake, and inexact modification of the two-dimensional loading for three-dimensional flow. Rowe[21] has shown that large changes in calculated flutter speed result when the loading applied to struts is modified to simulate cavitation. Available observations are insufficiently detailed to confirm the existence of the

---

[21]Rowe, W. S. and T. G. B. Marvin, "A Program of Theoretical Research on Hydroelastic Stability," The Boeing Company, Contract N00014-67-C-0248 (Nov 1968).

assumed distributions of cavitation. It has been shown[22] that altering boundary layer characteristics with disturbance wires affects agreement between theoretical and experimental loading in two-dimensional flow. However, the results of such modification on flutter characteristics have not been investigated. Reliable measurements of three-dimensional strut loading which could be used to assess the accuracy of the strip theory employed in the present flutter analysis are not available.

The existence of two different unstable hydroelastic modes implies that future flutter experiments and calculations must be carried out in sufficient detail to distinguish between the modes. This will require measurement or calculation of hydroelastic mode characteristics as a function of speed. Measurements of damping characteristics at zero speed are important, particularly for struts which undergo torsional flutter, so that calculated damping can be adjusted to include structural damping.

Flutter research will be incomplete until hydroelastic mode characteristics of full-scale strut systems are measured. These measurements will provide comparisons with model data and calculations as well as indicate the stability of the actual struts.

DESIGN PROCEDURES

Design of inverted-T strut-foil systems to operate in subcavitating flow can be based on the flutter-free performance of the existing U. S. Navy hydrofoil craft. In order to estimate the effect of variations in configuration, it would be helpful to calculate the hydroelastic mode characteristics and the generalized mass ratio of existing struts for comparison with parametric trends obtained from models. Further model testing may be required to establish stability criteria in areas where theory and present data are inadequate, such as in the presence of cavitating flow.

---

[22]Greidanus, J. H. et al., "Experimental Determination of the Aerodynamic Coefficients of an Oscillating Wing in Incompressible Two-Dimensional Flow, Part I, Wing with Fixed Axis of Rotation," Report F101, National Aeronautical and Astronautical Research Institute, Amsterdam (1952).

Additional information about hydroelastic stability can be obtained by flutter testing a reduced-scale model of a proposed design. The model should be dynamically and geometrically scaled, except for sweep angle. It has been found to be virtually impossible to obtain flutter in a low density strut model at small sweep angles prior to structural failure due to approaching divergence. Instead of testing the model at the small sweep angle usually found on full-scale struts, the model should be tested at several larger sweep angles, decreasing the angle until static deflections indicate proximity to divergence. Flutter speeds must then be extrapolated to the required value of sweep angle.

Damping and frequency measurements for individual hydroelastic modes of torsion-type struts have been readily obtained at NSRDC by impulsive excitation. This technique involves inducing oscillation of the strut at the desired frequency, and determining damping and frequency from the resulting decaying oscillations. Excitation was obtained from a vibration generator rapidly swept over a narrow frequency interval including the desired resonance. The technique can be applied at small speed increments to permit a close approach to the flutter inception speed to be made safely. It has been found, however, that at speeds above flutter inception struts often exhibit amplitude-limited flutter over a varying speed range before large negative damping leads to large amplitude oscillations. Because of the differences in damping characteristics, amplitude-limited bending flutter occurs over a narrow speed range while amplitude-limited torsional flutter can occur over a wide speed range. This phenomenon probably resulted in the failure of Model 2T, pod configuration D, shown in Figure 3 at a speed far above flutter inception.

Development of flutter testing techniques for full-scale craft would permit verification of the stability of a given design. Such techniques should be evaluated in models and on existing craft. Future designs could provide for the flutter testing system to be installed in all craft during construction to make underway flutter testing routine for hydrofoil vessels.

CONCLUSIONS

Strut flutter occurs in two different hydroelastic modes. At low values of generalized mass ratio, flutter occurs in a predominantly first bending mode shape with the qualitative characteristics of the "new mode" previously described. At higher values of generalized mass ratio, flutter occurs in a predominantly first torsion mode shape with the qualitative characteristics of "mode 2" described in the text. The flutter mode of a strut can be determined by examining the mode shape of the second vibration mode of a strut in water, except in a transition region where strong coupling interferes with this identification.

Flutter speed predictions using the present analysis are generally inaccurate. In the bending flutter region, flutter is often predicted to occur in the wrong mode so that flutter speed predictions cannot be used. In the torsional flutter region, the accuracy of flutter speed predictions is dependent on the value of torsional mass ratio. Predicted mode shapes and frequencies are nearly always accurate when three-dimensional hydrodynamic loading is used.

Foils attached to a strut in an inverted-T configuration have a strong effect on the flutter characteristics of the strut. Further investigation of foil effects is needed.

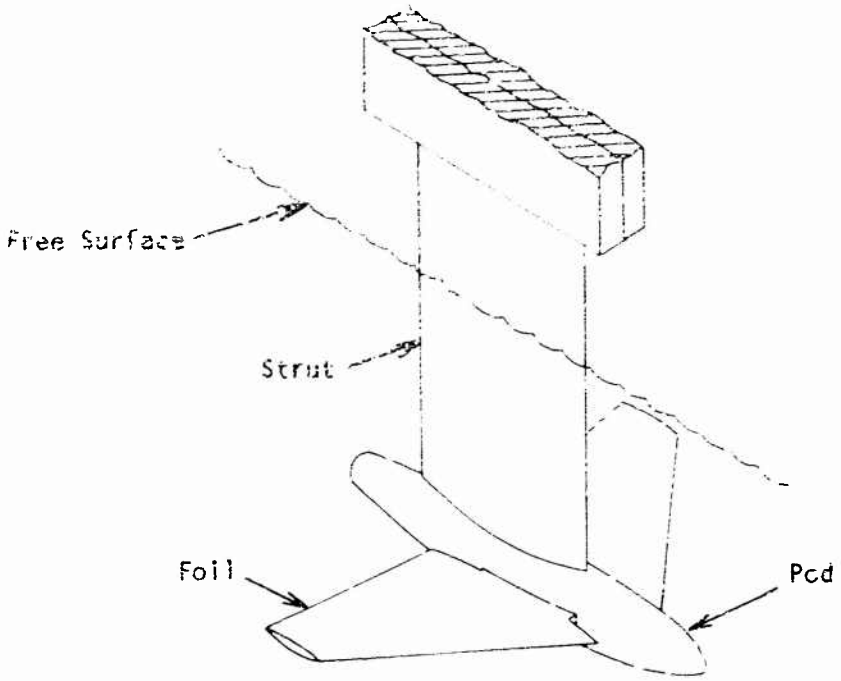

Figure 1 - Typical Strut-Pod-Foil System

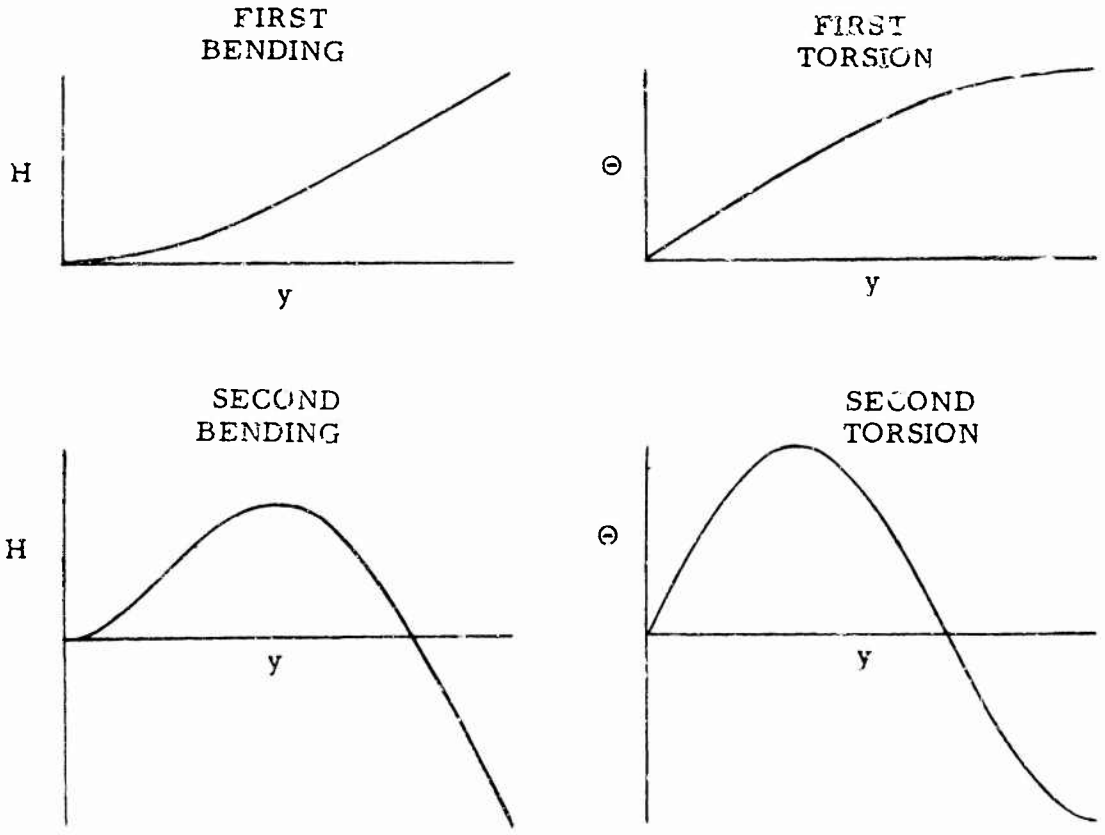

Figure 2 - Uncoupled Mode Shapes of Cantilever Beam

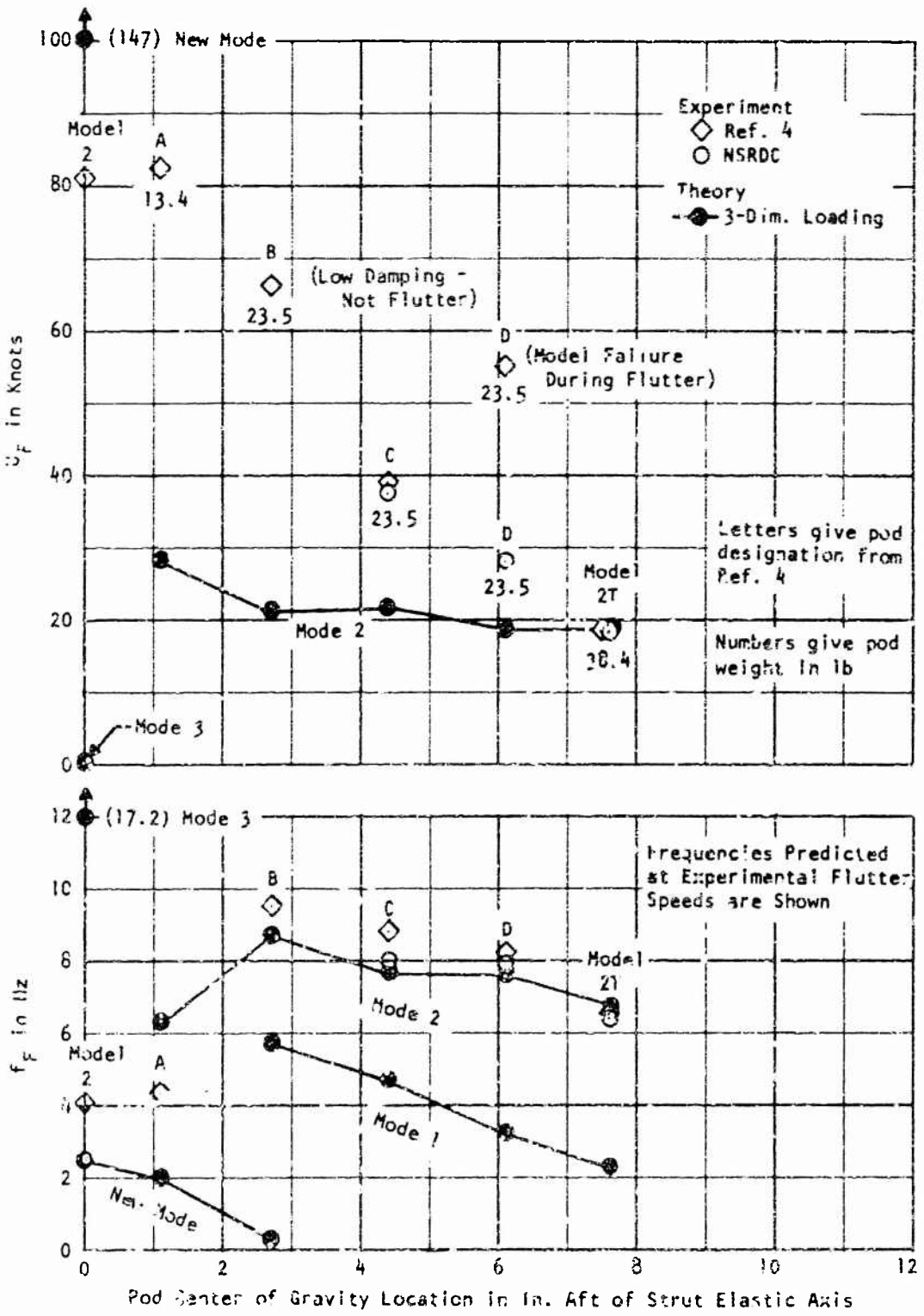

Figure 3 - Effect of Pod Mass and Center of Gravity Location on Flutter Speed U_F and Flutter Frequency f_F

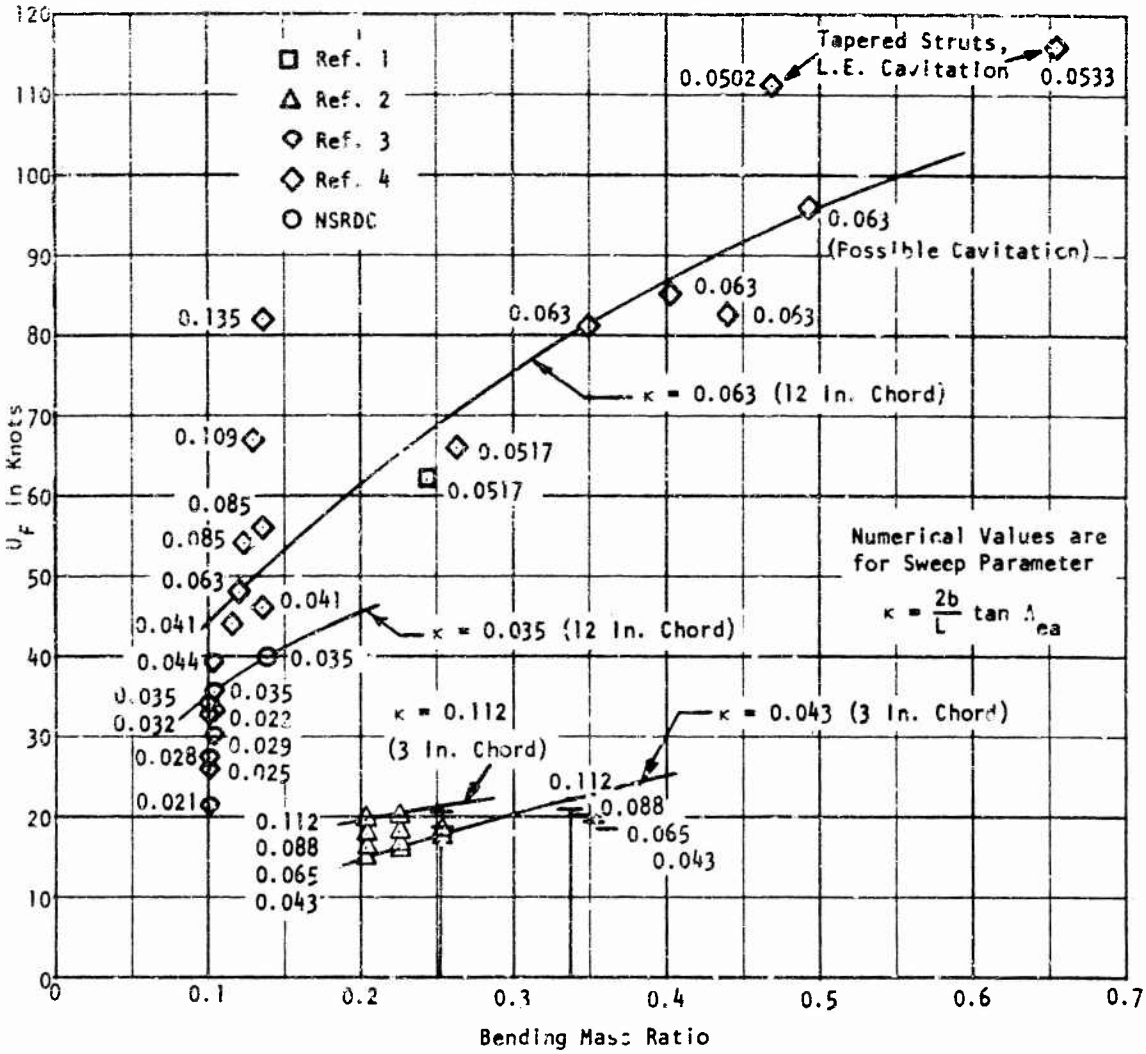

Figure 4 - Experimental Flutter Speed U_F as a Function of Bending Mass Ratio for Bending-Type Struts

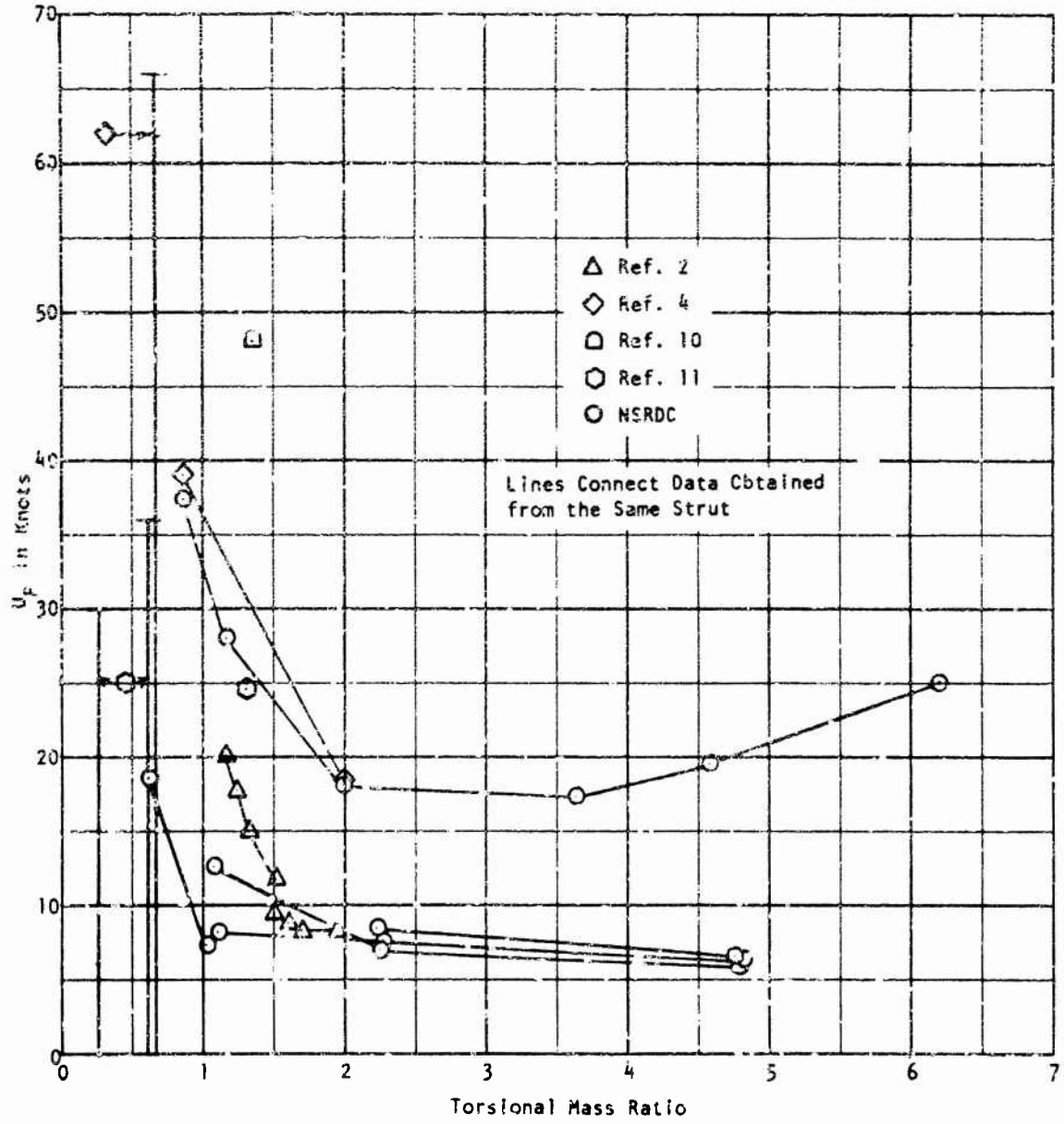

Figure 5 - Experimental Flutter Speed U_F as a Function of Torsional Mass Ratio for Torsion-Type Struts

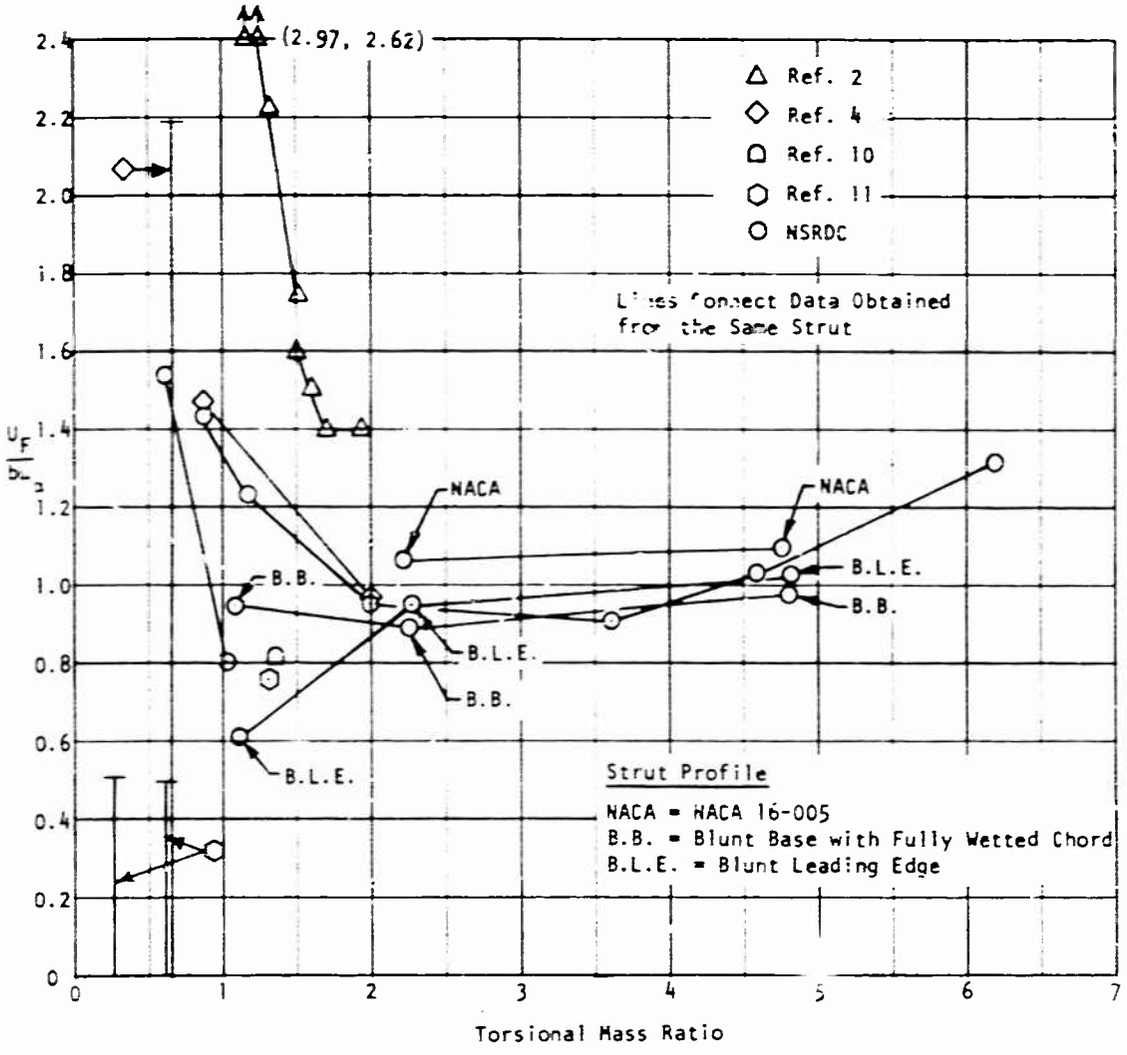

Figure 6 - Reduced Flutter Speed $U_F/b\omega_\alpha$ as a Function of Torsional Mass Ratio for Torsion-Type Struts

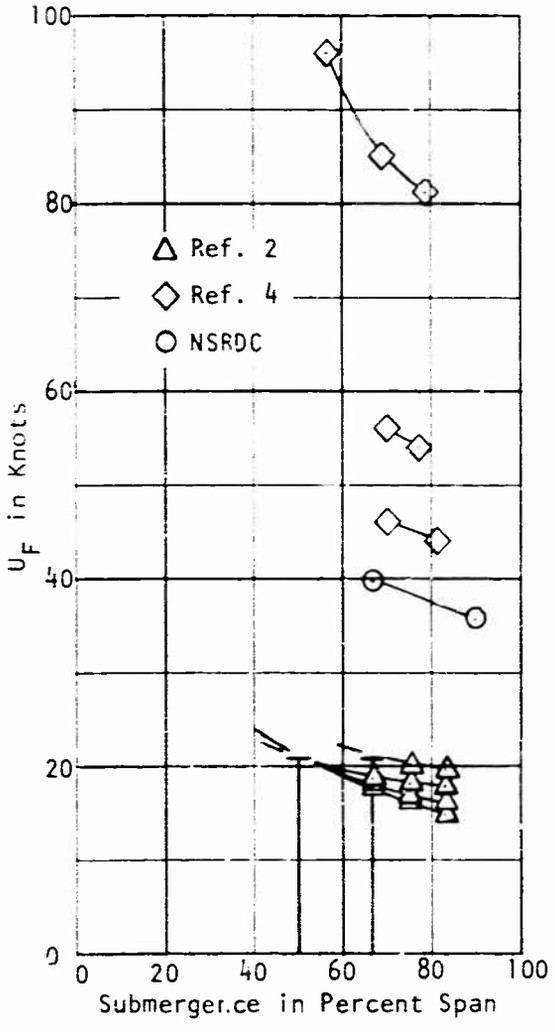

Figure 7a - Strut Models
(Bending-Type)

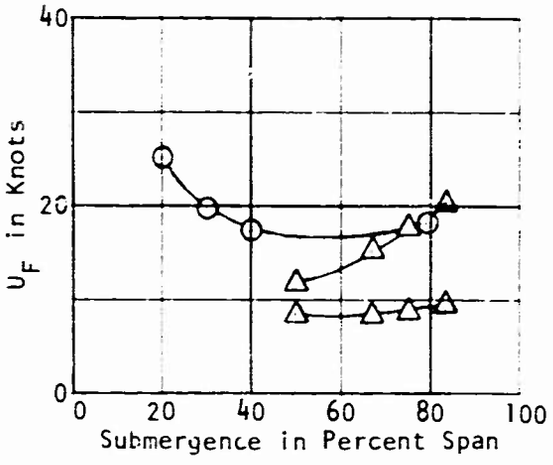

Figure 7b - Strut-Pod Models
(Torsion-Type)

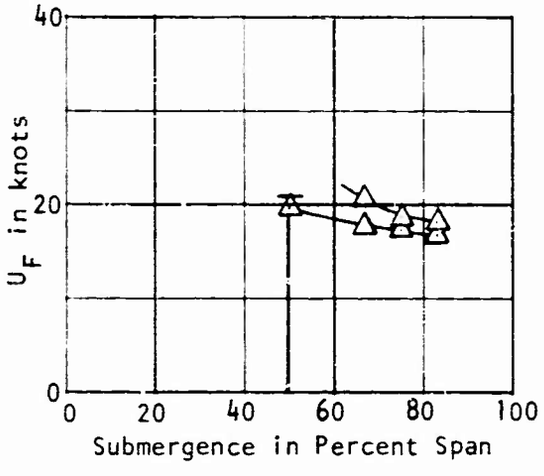

Figure 7c - Strut with Pod
and Foils

Figure 7 - Comparison of the Effect of Strut Submergence on Flutter Speed U_F for Strut Models with and without Pods and Foils

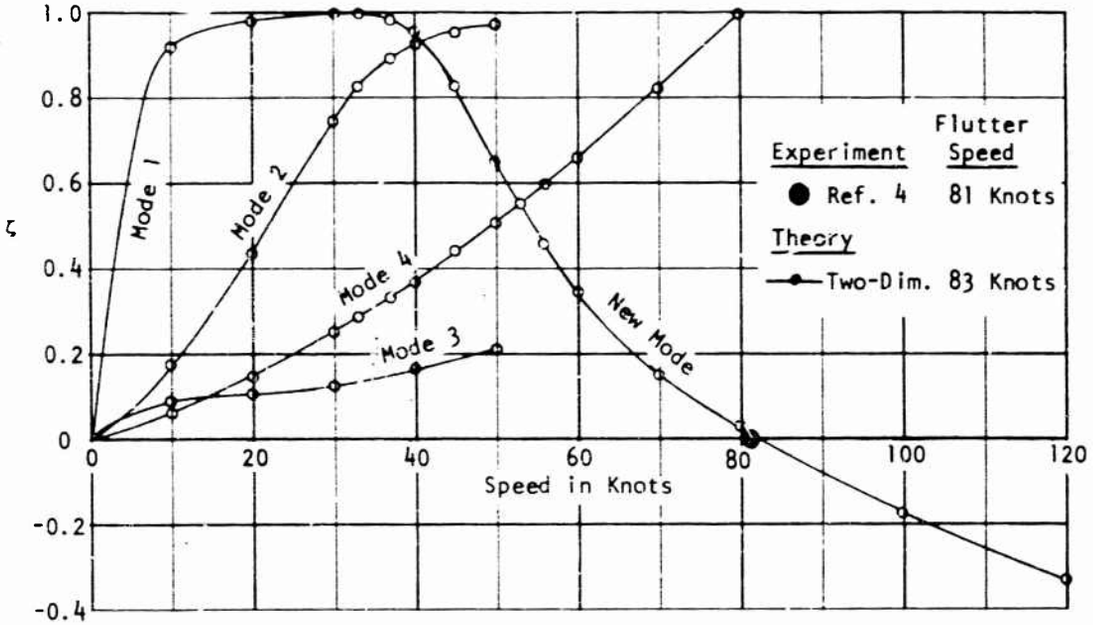

Figure 8a - Damping Ratio ζ

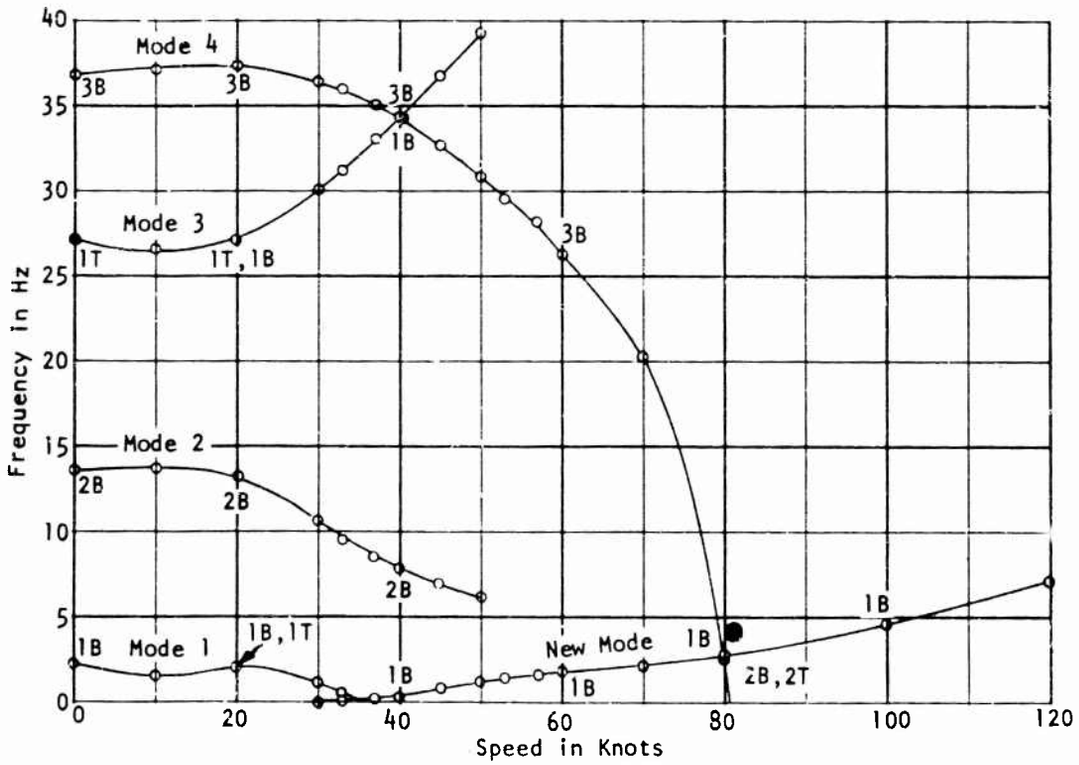

Figure 8b - Frequency

Figure 8 - Hydroelastic Mode Characteristics for Model 2
(Two-Dimensional Loading Calculation)

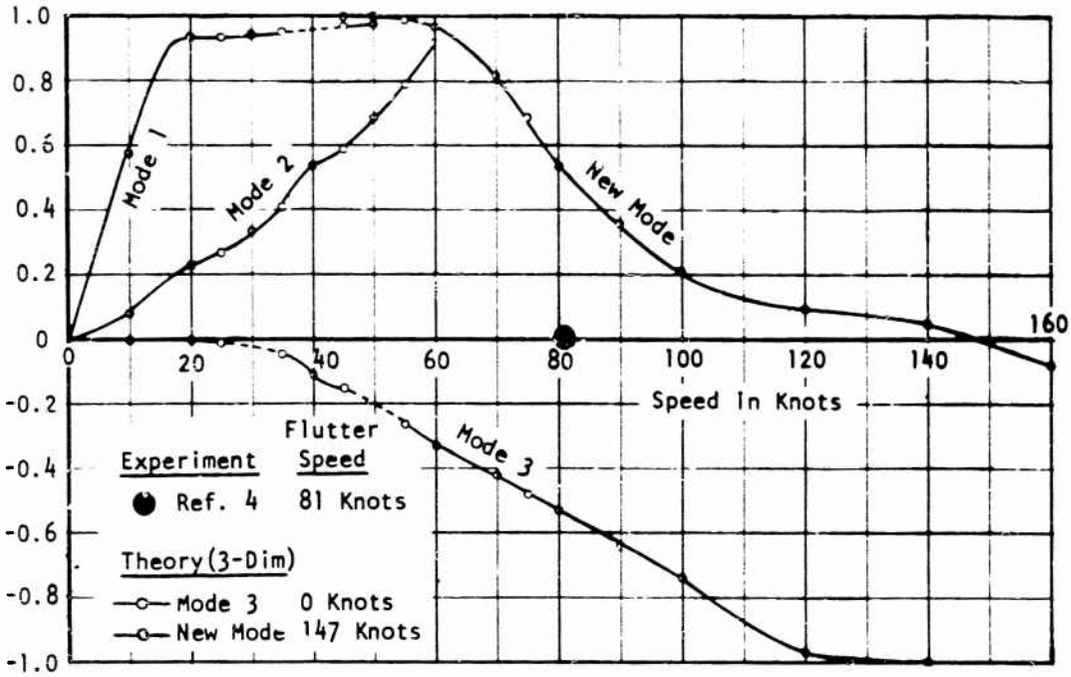

Figure 9a - Damping Ratio ζ

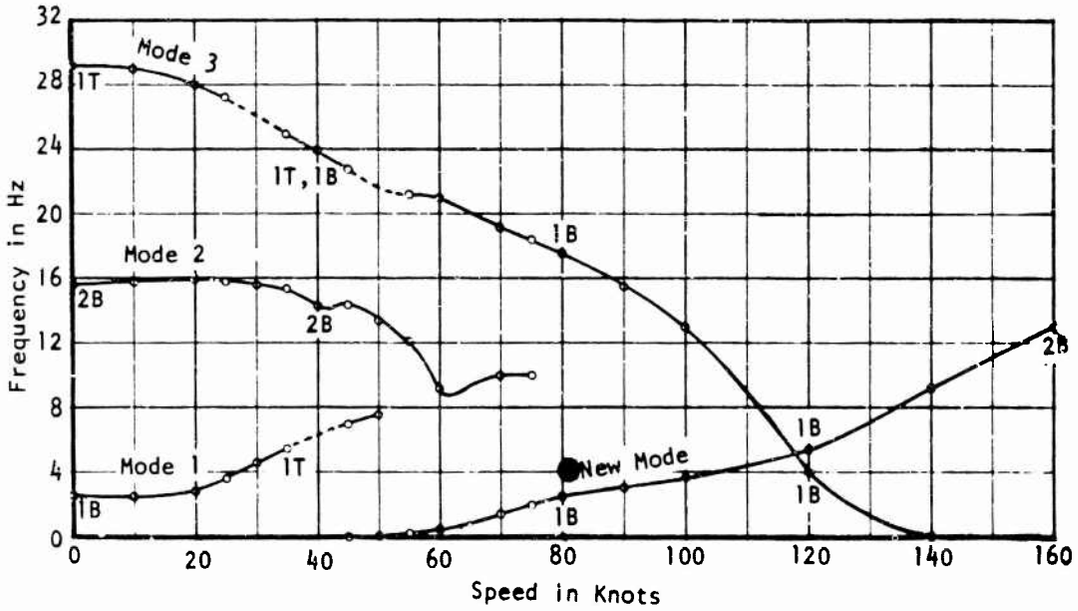

Figure 9b - Frequency

Figure 9 - Hydroelastic Mode Characteristics for Model 2
(Three-Dimensional Loading Calculation)

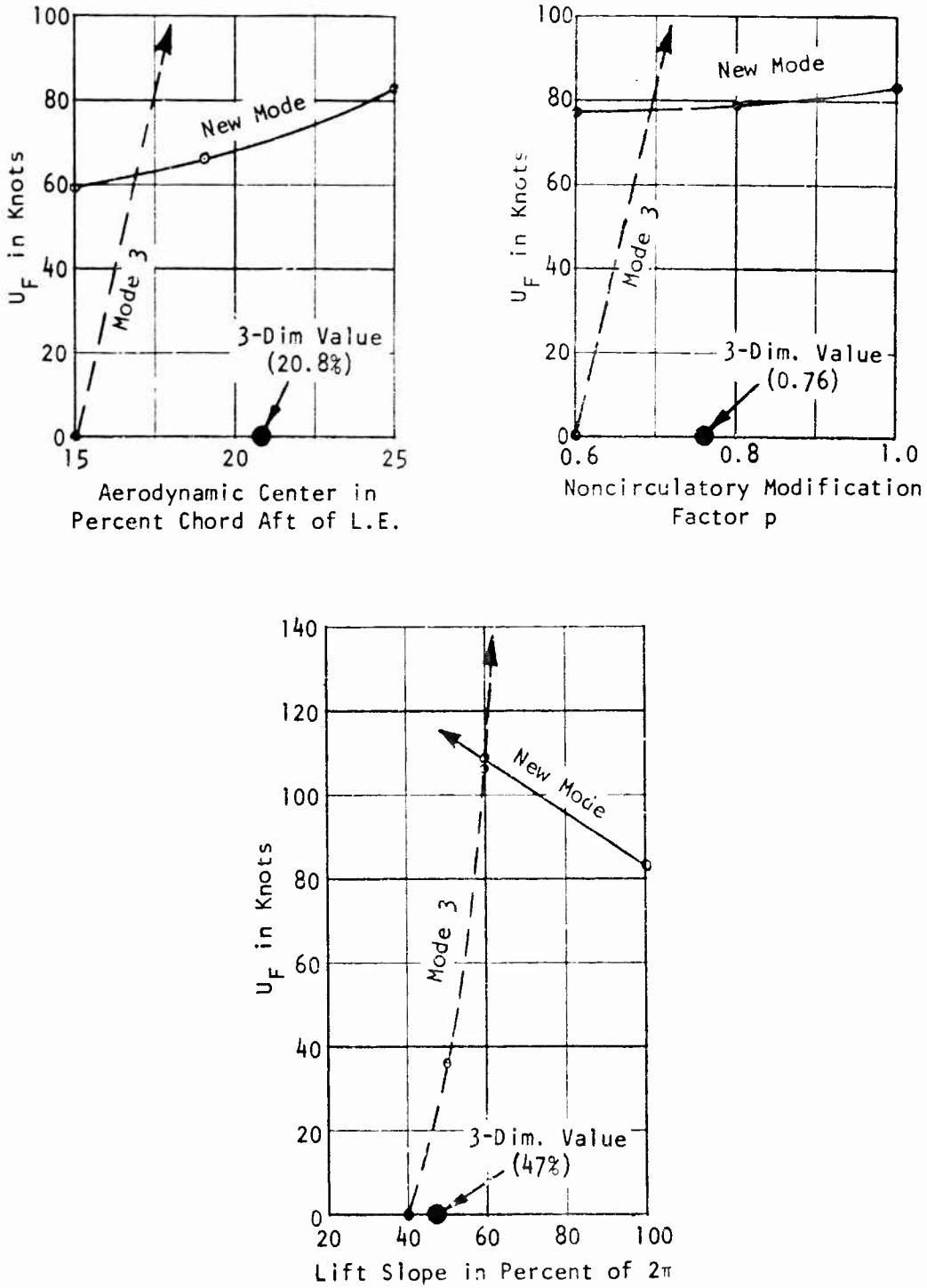

Figure 10 - Effect of Loading Modifications on Calculated Flutter Speed U_F for Model 2

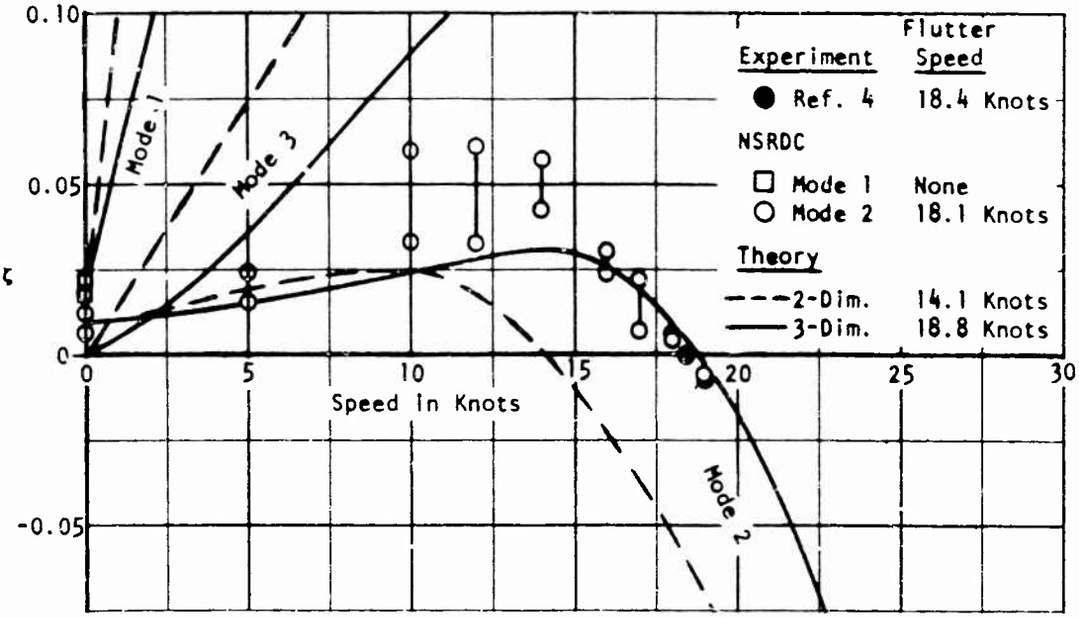

Figure 11a - Damping Ratio ζ

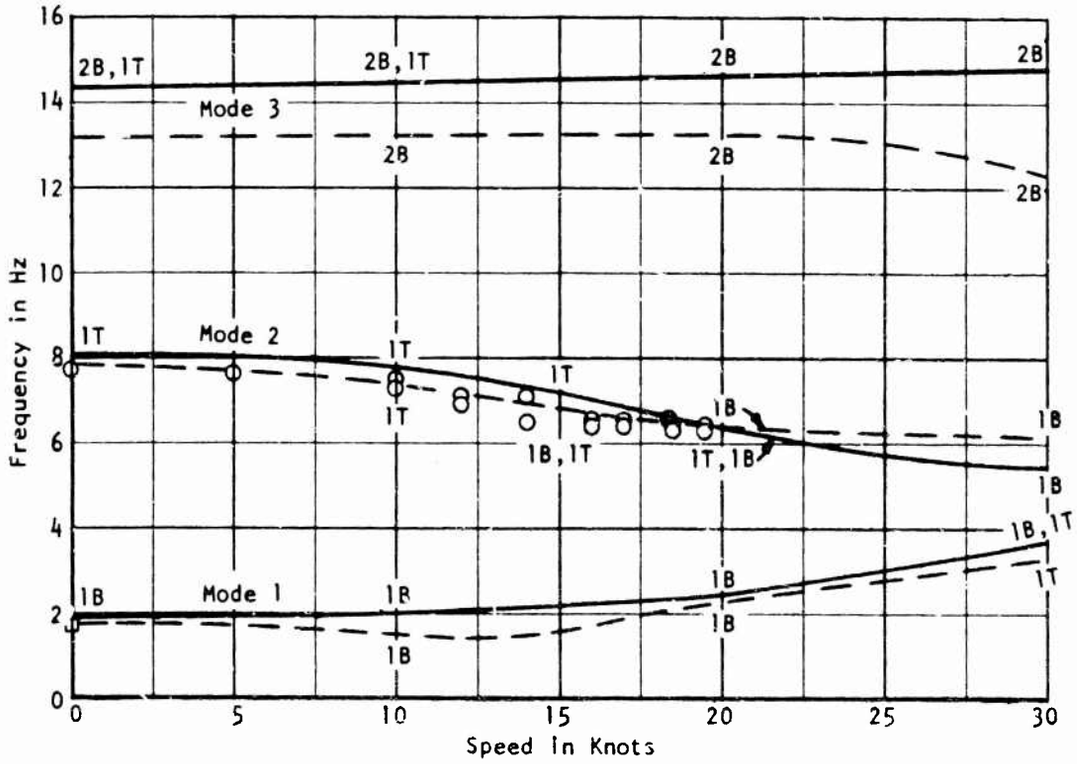

Figure 11b - Frequency

Figure 11 - Hydroelastic Mode Characteristics for Model 2T

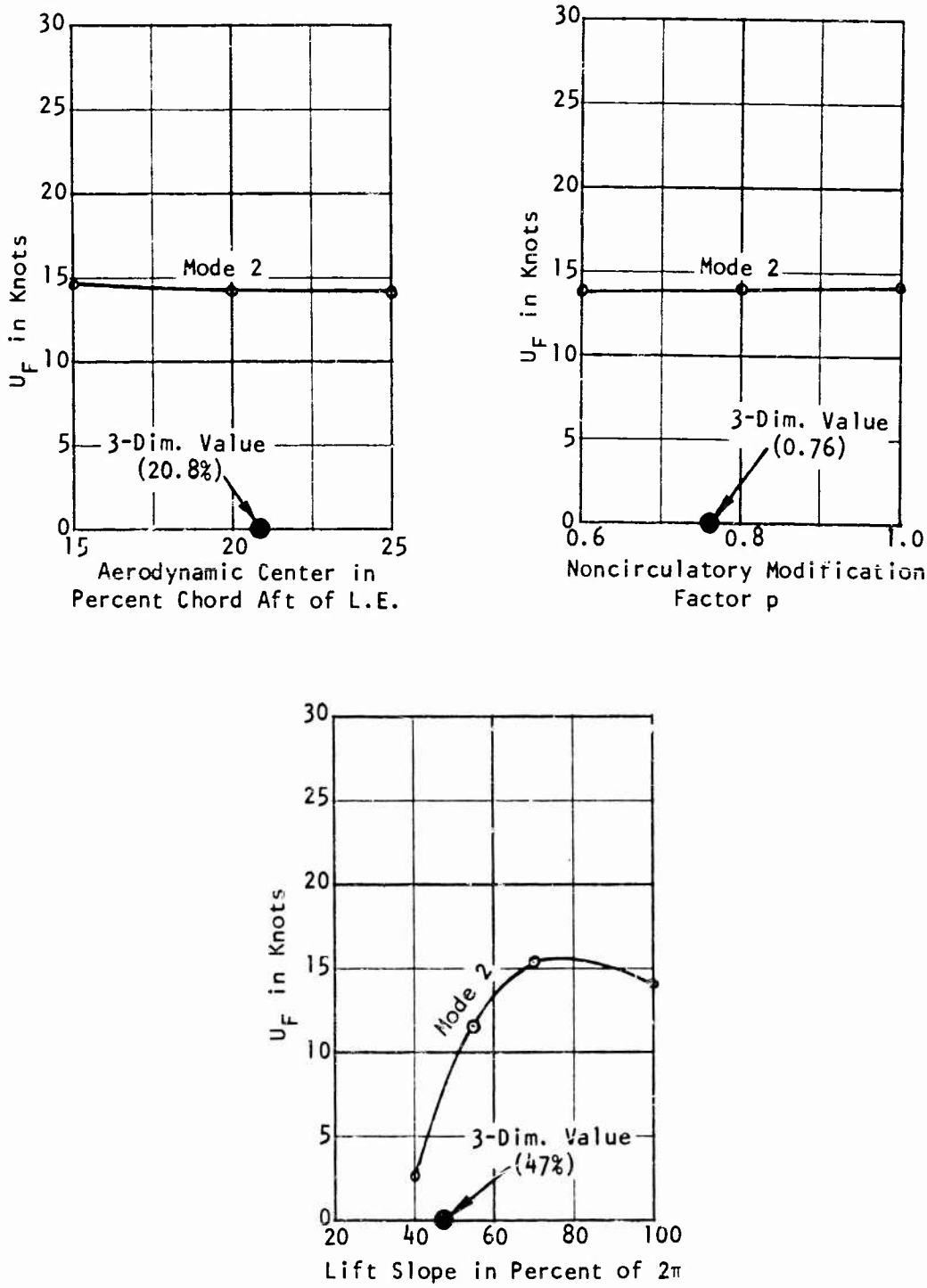

Figure 12 - Effect of Loading Modifications on Calculated Flutter Speed U_F for Model 2T

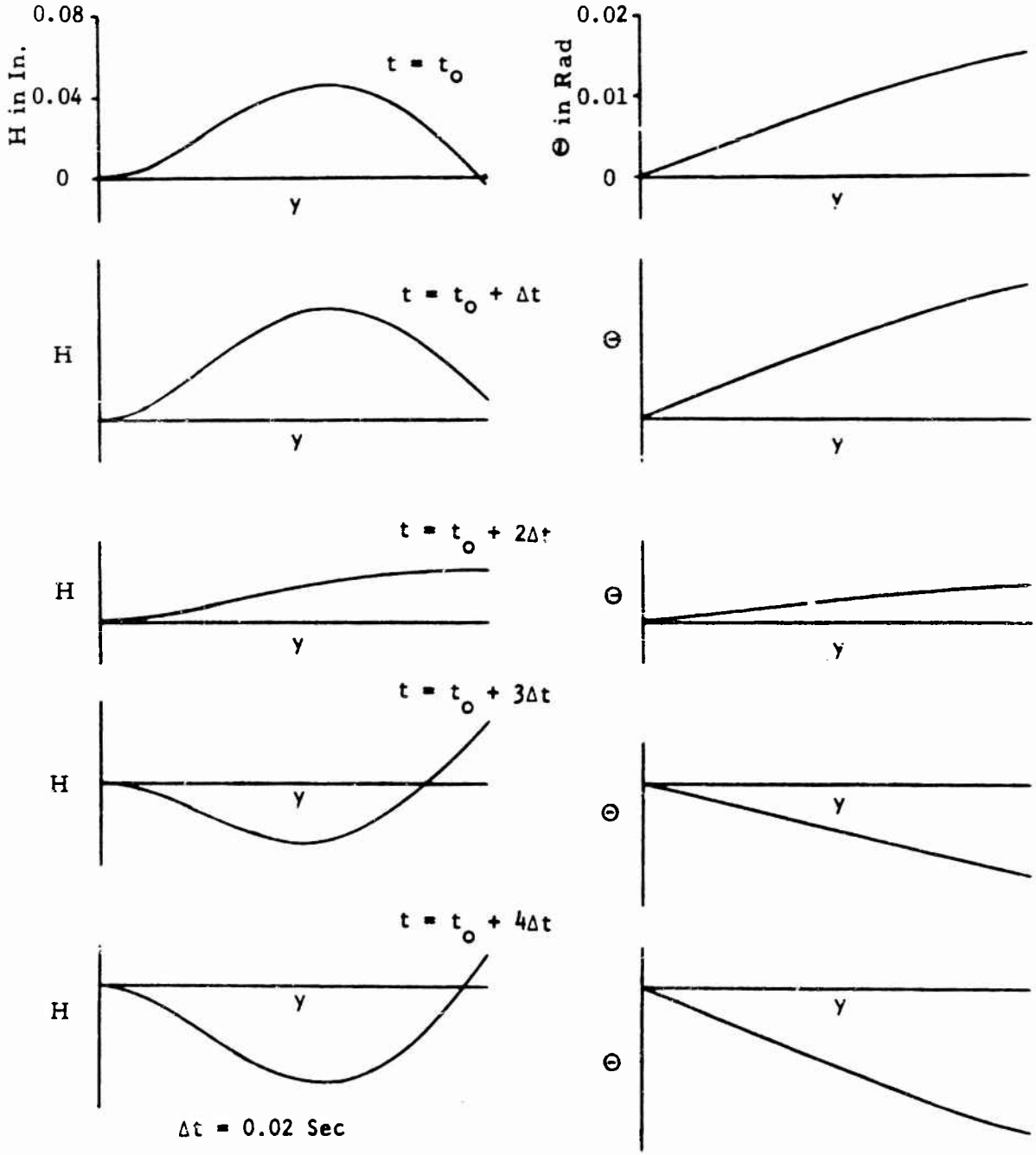

Figure 13 - Calculated Transient Response for Model 2T at Flutter

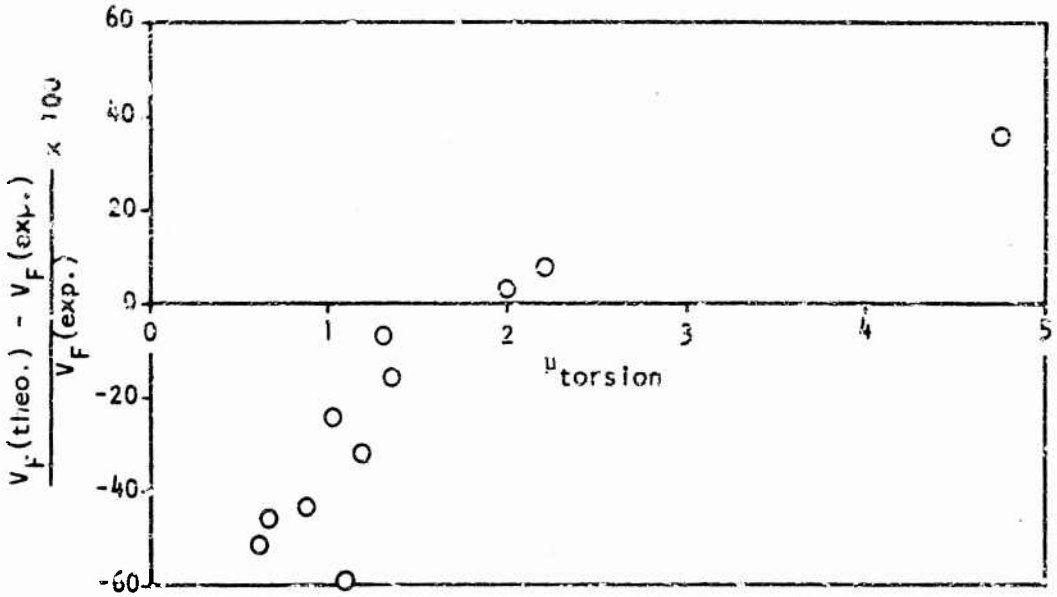

Figure 14 - Comparison of Experimental and Theoretical Flutter Speeds for Torsion-Type Struts without Foils

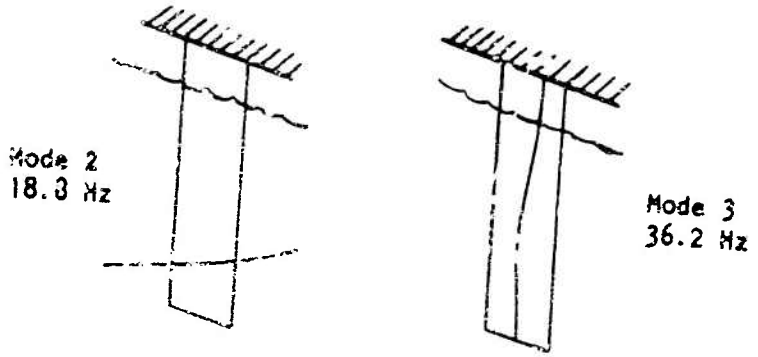

Figure 15a - Strut

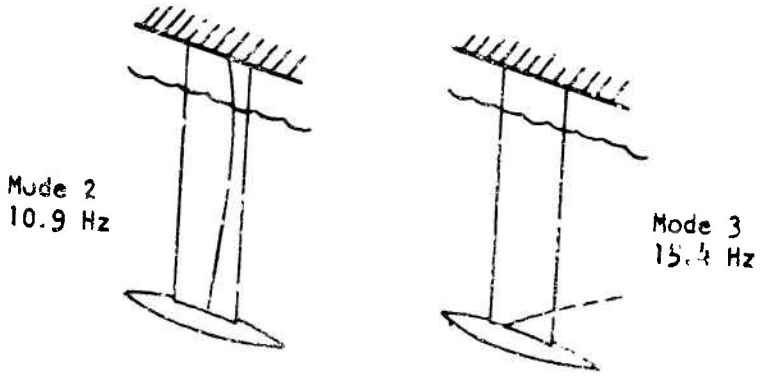

Figure 15b - Strut with Pod

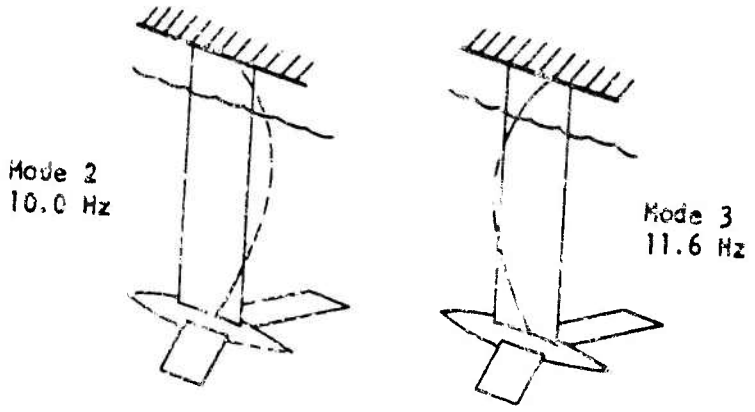

Figure 15c - Strut with Pod and Foils

Figure 15 - Calculated Nodal Lines for Strut of Reference 2 at 83 Percent Submergence in Water

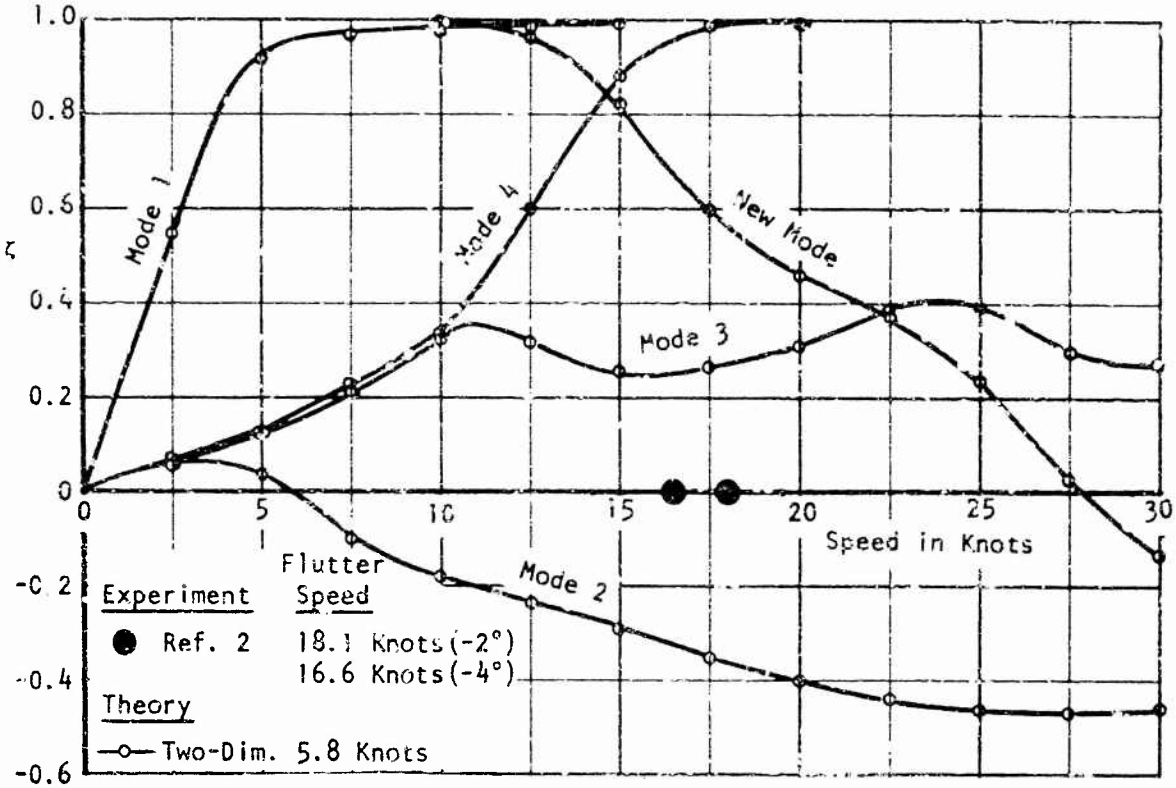

Figure 16a - Damping Ratio ζ

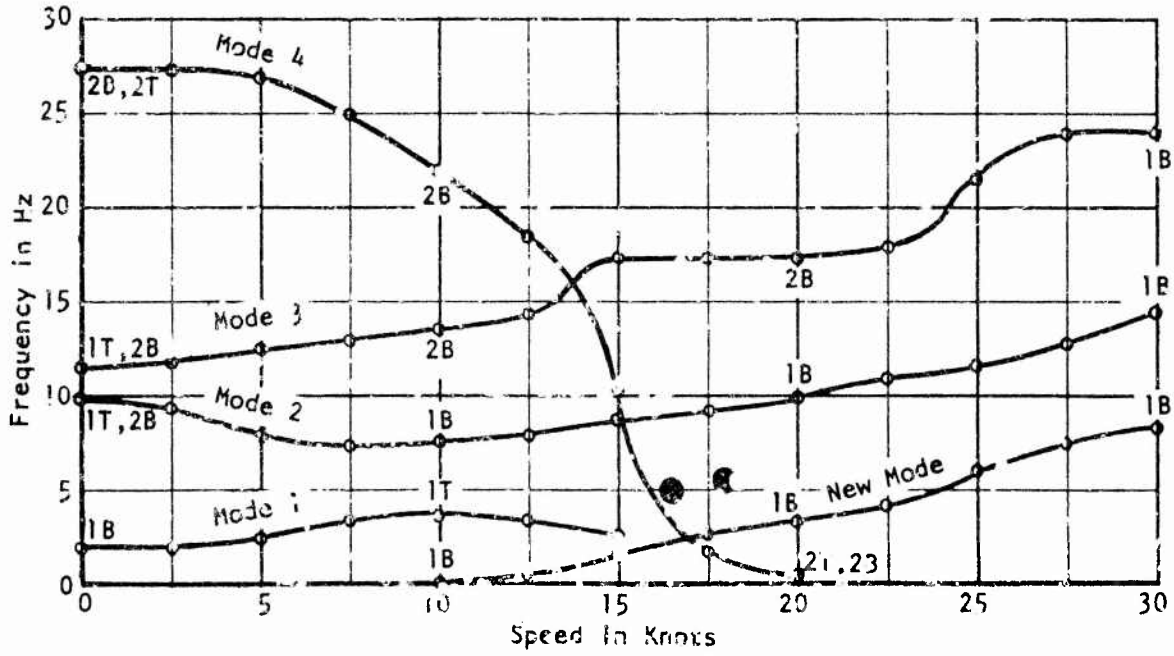

Figure 16b - Frequency

Figure 16 - Hydroelastic Mode Characteristics for Strut of Reference 2 with Pod and Foils (Two-Dimensional Loading Calculation)

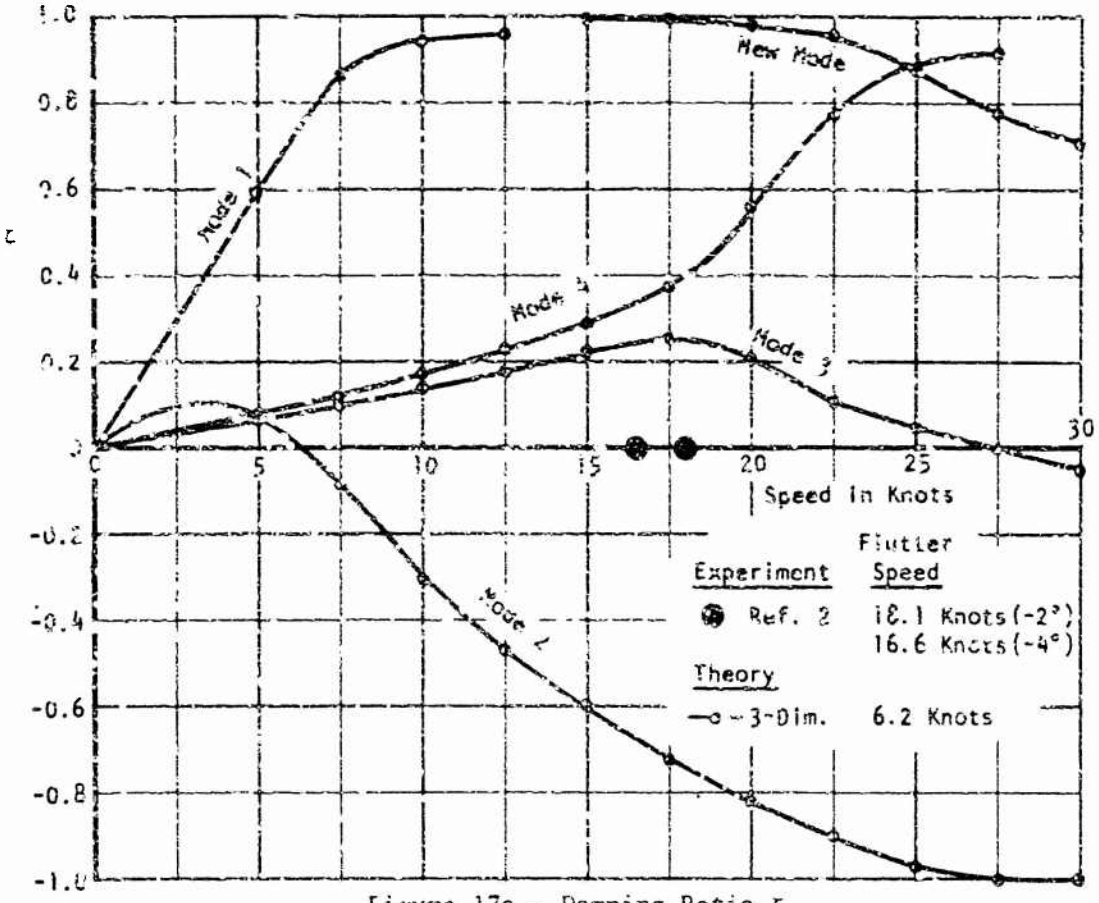

Figure 17a - Damping Ratio ζ

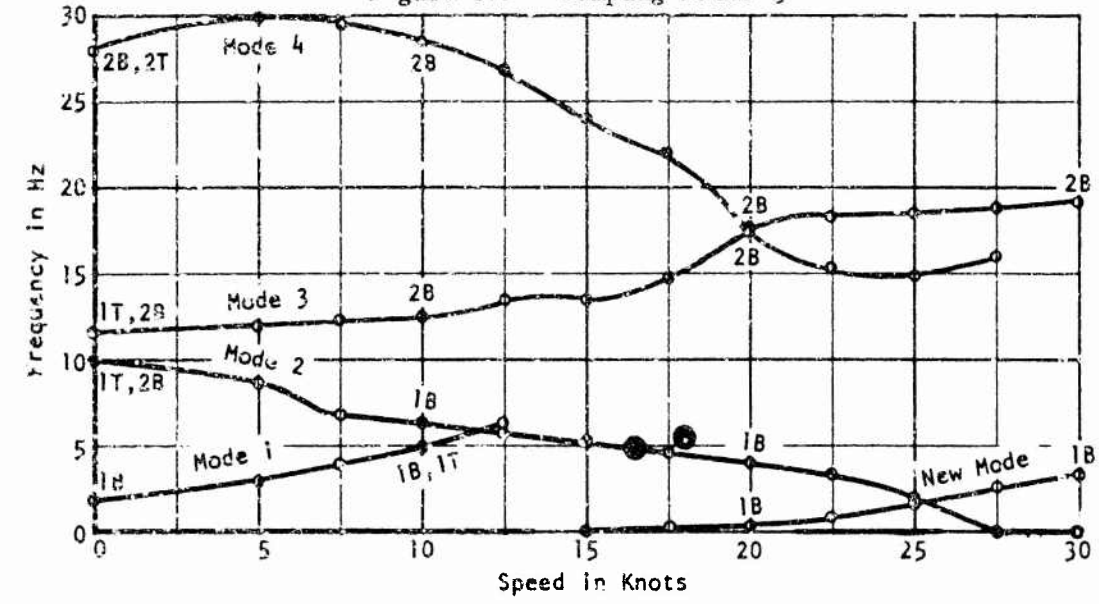

Figure 17b - Frequency

Figure 17 - Hydroelastic Mode Characteristics for Strut of Reference 2 with Pod and Foils (Three-Dimensional Loading Calculation)

APPENDIX

DESCRIPTION OF STRUT MODELS

MODEL 2

Model 2 was a blunt-based strut[4] constructed of solid steel. Its dimensions are shown in Figure 18, and its structural characteristics are summarized in Table 1. Spanwise distributions of lift slope, aerodynamic center, and noncirculatory modification factor are shown in Figure 19.

TABLE 1 - STRUCTURAL CHARACTERISTICS OF MODEL 2

Model Parameter	Value
L in in.	49.693
Λ_{ea} in deg	15
b in in.	5.796
m in lb-sec^2/in.^{2}	0.00273
a	0.38
x_α	- 0.214
I_α in lb-sec^2-in.	1.488
EI in lb-in.^{2}	1.293 x 10^6
GJ in lb-in.^{2}	2.070 x 10^6

MODEL 2T

Model 2T was constructed to the same specifications as Model 2, except that a 2-in. diameter pod was welded to its tip.[4] Pod dimensions are shown in Figure 20. Weights were placed in the body of the pod to produce different inertial configurations.

STRUT-FOIL MODEL

The strut[2] consisted of a solid bar of copper alloy covered with flexible silicone rubber. The leading edge of the strut was coated with a thin layer of plastic which was slit to reduce its stiffening effect. The strut profile closely resembled that of Models 2 and 2T, except for a rounded leading edge. Strut dimensions are shown in Figure 21. Structural characteristics are given in Table 2. The three-dimensional loading curves for this strut were essentially the same as those for Model 2, differing only in sweep angle.

TABLE 2 - STRUCTURAL CHARACTERISTICS OF STRUT OF REFERENCE 2

Model Parameter	Value
L in in.	12
Λ_{ea} in deg	15
b in in.	1.449
m in lb-sec^2/in.^{2}	1.0363×10^{-4}
Strut weight in lb	0.48
Pod and foils weight in lb	0.73
a	0.38
x_α	- 0.214
I_α (strut) in lb-sec^2-in.	8.525×10^{-4}
EI* in lb-in.^{2}	383
GJ* in lb-in.^{2}	614
*Note: 0.67 of Reference 2 value	

The pod and foils were machined from solid aluminum and were attached to the strut with bolts. Dimensions for these components are given in Figure 22.

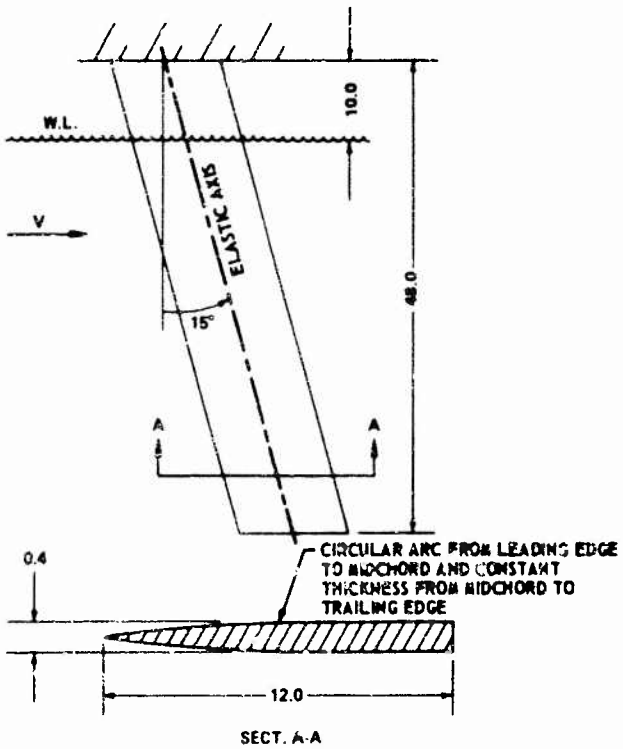

Figure 18 - Model 2 Dimensions

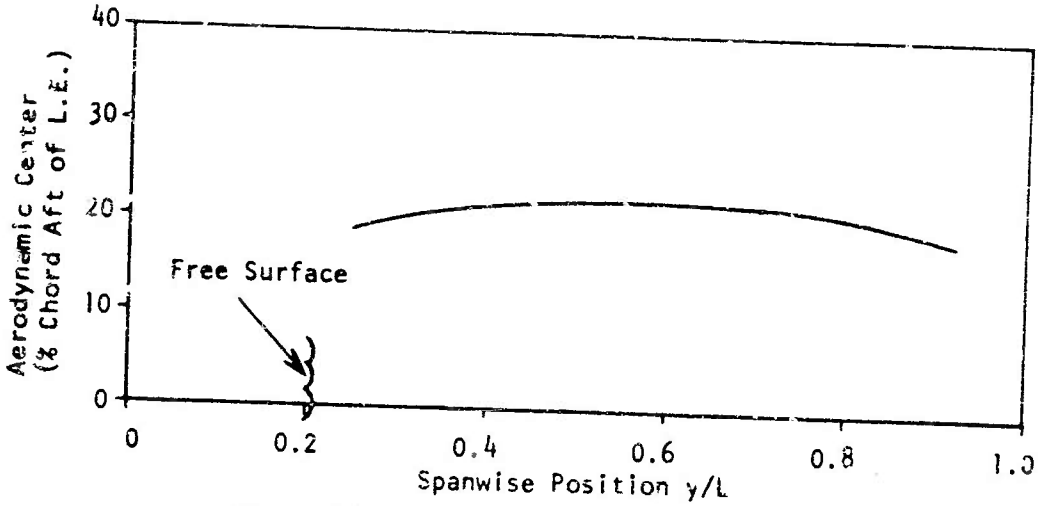

Figure 19a - Aerodynamic Center Location

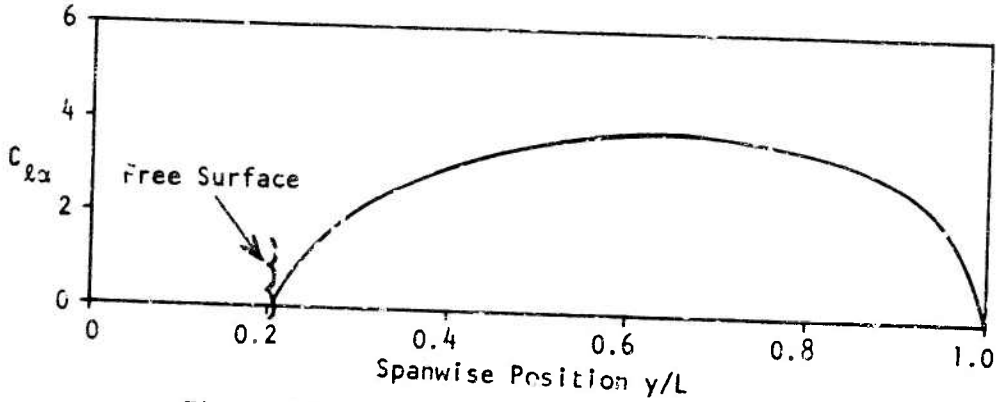

Figure 19b - Local Lift Coefficient Slope $C_{\ell\alpha}$

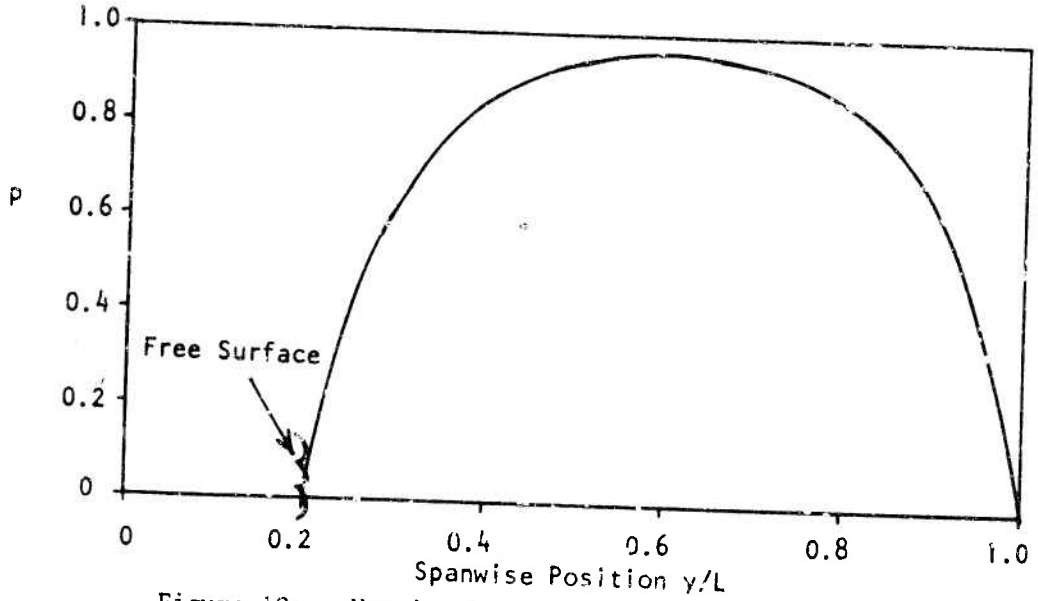

Figure 19c - Noncirculatory Modification Factor p

Figure 19 - Spanwise Distributions of Loading Modification Parameters

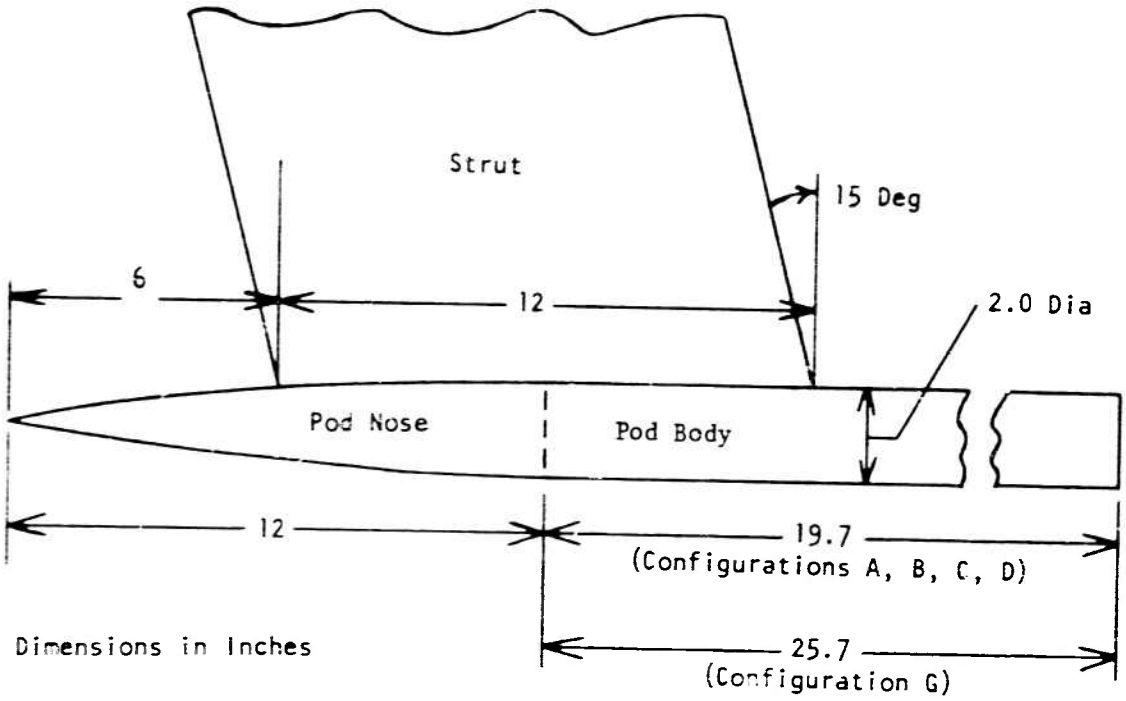

Figure 20 - Pod Used on Model 2T

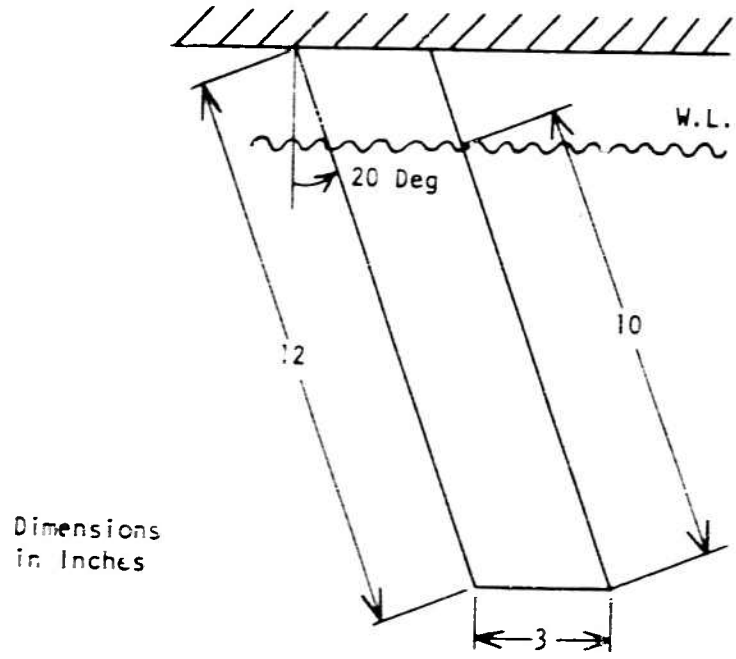

Figure 21 - Strut Used with Pod and Foils
(Reference 2)

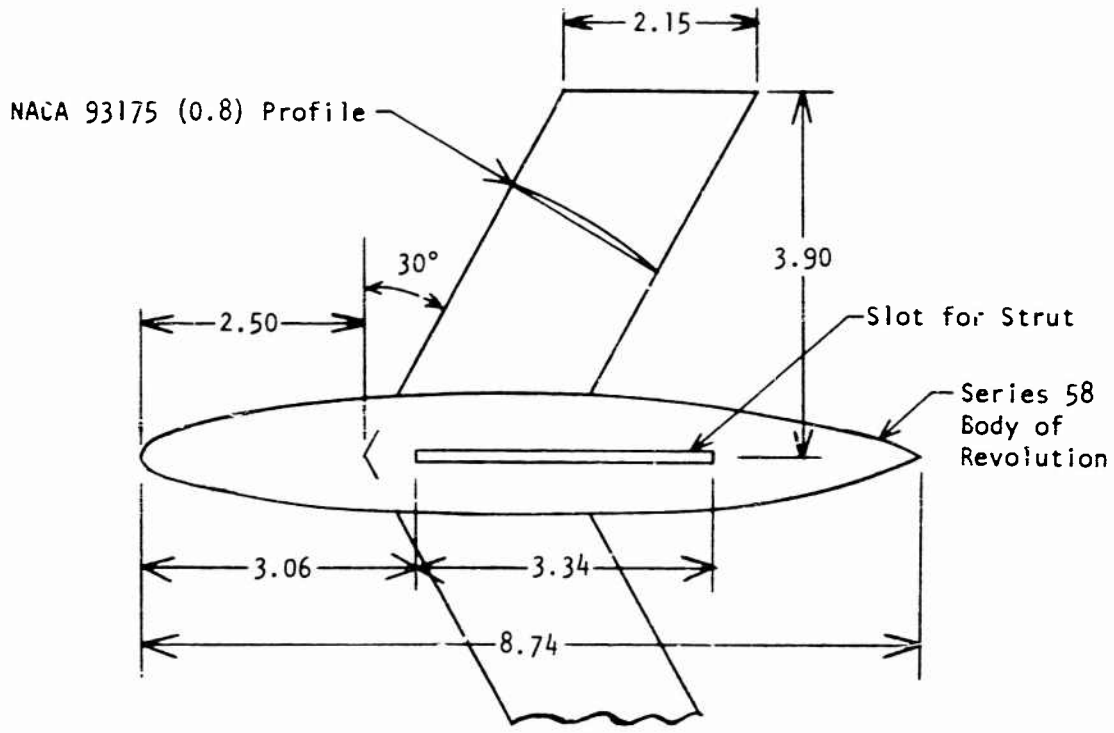

Dimensions in Inches

Figure 22 - Pod and Foil Attachment for Strut of Reference 2

REFERENCES

1. Hillborne, D. V., "The Hydroelastic Stability of Struts, Admiralty Res. Lab. Report No. ARL/R1/G/HY/5/3 (1958).

2. Huang, T. T., "Experimental Study of a Low Modulus Flutter Model for Strut-Foil-Pod Configurations," Hydronautics, Inc. Technical Report 459-2 (Jul 1967).

3. Squires, C. E., Jr., "Hydrofoil Flutter, Small Sweep Angle Investigation - Final Report," Grumman Aircraft Engineering Corporation Report DA Nonr-3989.3 (Nov 1963).

4. Baird, E. F. et al., "Investigation of Hydrofoil Flutter - Final Report," Grumman Aircraft Engineering Corporation Report DA 10-480-3 (Feb 1962).

5. Jordan, P. F., "On the Flutter of Swept Wings," Journal of the Aeronautical Sciences, Vol. 24, No. 3, pp. 203-210 (1957).

6. Caporali, R. L. and E. J. Brunelle, "Hydrofoil Instability at Low Mass Density Ratios, Princeton University Aerospace and Mechanical Sciences Report No. 670 (Mar 1964).

7. Herr, R. W., "A Study of Flutter at Low Mass Ratio with Possible Application to Hydrofoils," NASA TN-D-831 (May 1961).

8. Squires, C. E., Jr. and E. F. Baird, "The Flutter Characteristics of a Hydrofoil Strut," Proceedings of the Fourth Symposium on Naval Hydrodynamics, pp. 739-759 (1962).

9. Ho, H. W., "The Development and Testing of Low Modulus Flutter Models of a Base-Vented Strut," Hydronautics, Inc. Technical Report No. 459-1 (May 1965).

10. Abramson, H. N. and G. E. Ransleben, Jr., "An Experimental Investigation of Flutter of a Fully Submerged Subcavitating Hydrofoil," Journal of Aircraft, Vol. 2, No. 5, pp. 439-442 (1965).

11. Besch, P. K. and Y. N. Liu, "Flutter and Divergence Characteristics of Four Low Mass Ratio Hydrofoils," Naval Ship Research and Development Center Report 3410 (Oct 1970).

12. Bisplinghoff, R. L. and H. Ashley, "Principles of Aeroelasticity," John Wiley and Sons, Inc., New York (1962), p. 235.

13. Wilkinson, J. H., "The Algebraic Eigenvalue Problem," Oxford University Press, New York (1965).

14. Yates, E. C., Jr., "Calculation of Flutter Characteristics for Finite-Span Swept or Unswept Wings at Subsonic and Supersonic Speeds by a Modified Strip Analysis," NACA RM L57L10 (1958).

15. Liu, Y. N. and P. K. Besch, "Hydrofoil Flutter Analysis, Using a Modified Strip Theory," Naval Ship Research and Development Center Report 3624 (Jul 1971).

16. Yates, E. C., Jr., "Flutter Prediction at Low Mass-Density Ratios with Application to the Finite-Span Noncavitating Hydrofoil," AIAA Third Marine Systems and ASW Meeting (Apr-May 1968).

17. Ashley, H. et al., "New Directions in Lifting Surface Theory," AIAA Journal, Vol. 3, No. 1, pp. 3-16 (1965).

18. Dugundji, J. and N. Ghareeb, "Pure Bending Flutter of a Swept Wing in a High-Density, Low-Speed Flow," AIAA Journal, Vol. 3, No. 6, pp. 1126-1133 (1965).

19. Prasad, S. N. et al., "Bending-Torsional Flutter of a Swept Wing in a High-Density, Low-Speed Flow," AIAA Journal, Vol. 5, No. 2, pp. 316-321 (1967).

20. Peterson, L., "Theoretical Basis for SADSAM Computer Program," MacNeal-Schwendler Corporation Project Report (Dec 1970).

21. Rowe, W. S. and T. G. B. Marvin, "A Program of Theoretical Research on Hydroelastic Stability," The Boeing Company, Contract N00014-67-C-0248 (Nov 1968).

22. Greidanus, J. H. et al., "Experimental Determination of the Aerodynamic Coefficients of an Oscillating Wing in Incompressible Two-Dimensional Flow, Part I, Wing with Fixed Axis of Rotation," Report F101, National Aeronautical and Astronautical Research Institute, Amsterdam (1952).